

by the action of M6G [6]. In contrast, M3G decreases the analgesic activity of morphine and M6G [6]. Therefore, polymorphisms in the *UGT2B7* gene are associated with interindividual variability in the pharmacokinetics of morphine and its metabolites. Although the effects of genetic polymorphisms in *UGT2B7* on the pharmacokinetics of morphine and its efficacy in patients with cancer have been reported [7, 8], whether such polymorphisms influence morphine-related adverse reactions remains unclear.

Efflux transporter P-glycoprotein [ATP-binding cassette, sub-family B, member 1 (*ABCB1*)], coded by the *ABCB1* gene, is a major determinant of the intracellular concentration of morphine and its metabolites, M6G and M3G [9]. *ABCB1* can limit the entry of morphine and its metabolites into the brain and actively pump the drug out of the central nervous system. It is thus an important component of the blood–brain barrier [10]. So far, a variety of polymorphisms in the *ABCB1* gene have been identified [11]. Recently, Campa et al. [12] have shown that pain-relief variability in patients with cancer is significantly associated with 3435C > T in the *ABCB1* gene. This finding suggests that genetic variability of *ABCB1* may affect morphine disposition in the central nervous system. However, few studies have examined the relation between *ABCB1* genetic polymorphisms and morphine-induced adverse drug reactions in patients with cancer who receive morphine.

The primary site of action of morphine is the μ -opioid receptor, which is encoded by the *opioid receptor $\mu 1$* (*OPRM1*) gene. *OPRM1* is thus an initial candidate gene for studies evaluating the role of polymorphisms in the clinical response to morphine. A variety of polymorphisms have been identified in the *OPRM1* gene [13, 14]. The most prevalent polymorphism in the *OPRM1* gene is a nucleotide substitution 118A > G, causing amino acid change N40D at a putative *N*-glycosylation site in the extracellular region of the receptor. Recently, 118A > G was demonstrated to lower mRNA and functional protein expression in human brain tissue and in transfected cells [15]. To date, the association between single nucleotide polymorphism (SNP) and the efficacy of morphine has been relatively well investigated. Cancer patients homozygous for the G allele were found to be poor responders to morphine [12] and to require higher doses of morphine to relieve pain [16]. However, the association between 118A > G in *OPRM1* and morphine-induced adverse reactions in patients with cancer remains unclear.

We examined the effects of polymorphisms in the *UGT2B7*, *ABCB1*, and *OPRM1* genes on morphine-related adverse reactions in patients with cancer who received morphine therapy.

Methods

Materials

Morphine hydrochloride was kindly provided by Shionogi (Osaka, Japan). M3G, M6G, and naloxone hydrochloride were purchased from Sigma-Aldrich (St. Louis, MO, USA). All chemicals and solvents were of the highest grade commercially available.

Patients

Japanese patients with cancer who were receiving controlled-release morphine sulfate tablets (MS Contin, Shionogi, Osaka, Japan) to relieve cancer pain were enrolled. The protocols for the pharmacokinetic study of morphine and its metabolites and the pharmacogenetic study were approved by the Institutional Review Board of Saitama Medical University. All patients gave written informed consent for their peripheral blood samples and medical information to be used for research purposes.

Treatments

Controlled-release morphine sulfate tablets were orally administered to patients according to the standard protocol described in the package insert. When the initial dose was appropriate to relieve pain, the dose was determined as maintenance dose. If necessary, the initial morphine dose was modified to achieve the pain relief. When the pain was relieved enough by the modification of dose, the dose was determined as the maintenance dose. If patients did not tolerate with morphine treatment because of adverse events, the dose was adopted as maintenance dose. Thus, maintenance dose depended on the pain intensity of the patients and susceptibility of them to morphine. When the maintenance dose was obtained, morphine-induced adverse events were evaluated.

Morphine-induced adverse reactions

Morphine-induced adverse events, including constipation, nausea, vomiting, drowsiness/confusion, and fatigue, were evaluated according to the National Cancer Institute Common Toxicity Criteria (NCI-CTCAE), Version 3.0.

Genotyping

Genomic DNA was extracted from 200 μ l of peripheral blood, which had been stored at -80°C until analysis, with the use of a QIAamp Blood Kit (QIAGEN GmbH, Hilden, Germany).

UGT2B7 gene fragments containing 211G > T [rs12233719, A71S] and 802C > T [rs7439366, H268Y,

*UGT2B7**2] were amplified by polymerase chain reaction (PCR). Genomic DNA samples (100 ng) were added to the PCR mixtures (50 μ l), consisting of 1 \times PCR buffer, 3 mM MgCl₂ for 211G > T or 4 mM MgCl₂ for *2, 0.25 μ M of each primer, 200 μ M dNTPs, and 1.25 U of AmpliTaq Gold DNA polymerase (Applied Biosystems, CA, USA). The PCR primers used to amplify the *UGT2B7* gene fragments containing the respective polymorphisms were 2B7A71S-F (5'-TTAGTTTTGTGTCAATGGACTGCAGAAAC-3') and 2B7A71S-R (5'-AAATAAGTTAGAGCTTCATGTTACTGATTG-3') for 211G > T, and 2B7*2-F (5'-CTGTCAGGAAGACCCACTAC-3') and 2B7*2-R (5'-TTTACCTTAGGCAGGGGTTT-3') for 802C > T. All amplifications included a 15-min initial denaturation at 94°C. PCR was performed under the following conditions: 30 s at 94°C (40 s for *2), 40 s at 57°C (30 s at 56°C for *2), and 1 min at 72°C for 211G > T (30 s for *2) for 30 cycles, followed by a final extension at 72°C for 3 min. After the purification of the PCR products with QIAquick PCR purification kit (QIAGEN GmbH, Hilden, Germany), direct sequencing was performed with BigDye terminator var. 3.1 cycle sequencing kit and on a 3130 genetic analyzer (Applied Biosystems, CA, USA).

Gene fragments of *ABCB1* that included 1236C > T [rs1128503, G412G], 2677G > T, A [rs2032582, A893T, S], and 3435C > T [rs1045642, I1145I] were amplified by PCR. Forward and reverse primers used for PCR to amplify *ABCB1* gene fragments containing these polymorphic sites were ABCB1-1236F (5'-TGAATGAAGAGTTTCTGATGTTTCTTG-3') and ABCB1-1236R (5'-ATACATTTGTAATTGAAAGGGCAACAT-3'), ABCB1-2677F (5'-AATGAATATAGTCTCATGAAGGTGAGTTTT-3') and ABCB1-2677R (5'-CATCTTAGAGCATAGTAAGCAGTAGGG-3'), and ABCB1-3435F (5'-TGCGAGTTTCAGTGTAAAGAAATAATGA-3') and ABCB1-3435R (5'-TAATTTCTCTTCACTTCTGGGAGACC-3'), respectively. PCR was carried out in a total volume of 50 μ l in the presence of 100 ng of genomic DNA, 0.25 μ M each primer, 1 \times PCR buffer, 3 mM MgCl₂, 0.2 mM dNTPs, and 1.25 U of AmpliTaq Gold DNA polymerase. An initial denaturation at 94°C for 15 min was followed by 30 cycles of 0.5 min at 94°C, 40 s at 62°C, and 40 s at 72°C, as well as a final extension period of 3 min at 72°C. PCR products were sequenced directly as described above.

OPRM1 gene fragment containing 118A > G [rs1799971, N40D] was amplified by means of PCR. The forward and reverse primers used were 5'-TTTCCCTCCTCCCTCCCTTC-3' and 5'-GCCTTGGGAGTTAGGTGTCTCTTT-3', respectively. Genomic DNA samples (100 ng) were added to the PCR mixtures (50 μ l) consisting of 1 \times PCR buffer, 4 mM MgCl₂, 0.25 μ M of each primer, 200 μ M dNTPs, and 1.25 U of AmpliTaq Gold DNA polymerase. Amplification was performed by denaturation at 95°C for 30 s, annealing at 61°C for 40 s, and extension at 72°C for 1 min

for 30 cycles, followed by a final extension at 72°C for 3 min. PCR products were subsequently directly sequenced as mentioned above.

Determination of morphine, M6G, and M3G

Blood samples for pharmacokinetic analysis were obtained after oral administration of morphine. A blood sample was arbitrarily obtained during the period between one dose of morphine and the next dose. The samples were centrifuged immediately, and resulting plasma samples were stored at -80°C until analysis.

Plasma concentrations of morphine, M6G, and M3G were analyzed by reverse-phase high-performance liquid chromatography (HPLC). The HPLC system consisted of an EP-300 pump, ATC-300 column thermostat, EP-300 electron chemical detector (ECD), DG-300 degasser (Eicom, Kyoto, Japan), SIL-20A auto-sampler, SPD-10AVVP ultraviolet (UV) detector, and C-R6A Chromatopac (Shimadzu, Kyoto, Japan).

Morphine and M6G were analyzed with the use of an ECD and a SuperODS column (4.6 \times 100 mm, 2.3 μ m; Tosoh, Tokyo, Japan). The oxidation potential was 750 mV. The mobile phase was a mixture of 0.1 M phosphate buffer (pH 2.1) containing 30 μ M EDTA and 10 mM sodium dodecyl sulfate, acetonitrile, and methanol at a ratio of 90:8:2 (v/v). The column temperature was 40°C and the flow rate was 1.0 ml/min.

M3G was analyzed with the use of a UV detector and an L-column ODS (4.6 \times 250 mm, 5 μ m; Chemicals Evaluation and Research, Saitama, Japan). The wavelength of the UV detector was 210 nm, and the column temperature was 40°C. The mobile phase consisted of 0.1 M phosphate buffer (pH 2.1) containing 30 μ M EDTA and 10 mM sodium dodecyl sulfate, acetonitrile, and methanol at a ratio of 74:24:2 (v/v) and was delivered at a flow rate of 1.0 ml/min.

The lower limits of quantification were 67.2 pg/ml (236 pM) for morphine, 380 pg/ml (0.823 nM) for M6G, and 496 pg/ml (1.08 nM) for M3G.

Pharmacokinetic parameters

Individual oral clearances (l/h) of morphine were estimated by empirical Bayes estimates, based on a prior non-linear mixed effect analysis fit, using a 1-compartment model. Non-linear mixed effect analysis was performed with NONMEM program version VI (Globemax LLC, Hanover, MD, USA) to develop a population pharmacokinetic model.

Statistical analysis

Genotype and allele frequencies for each polymorphic allele in the respective genes were determined by using

SNPAlyze 5.1 (Dynacom, Yokohama, Japan). The significance of deviations from Hardy–Weinberg equilibrium was also tested with the program SNPAlyze 5.1. Linkage disequilibrium analysis to create a pairwise two-dimensional map of correlation coefficients r^2 and D' among SNPs in the *ABCB1* gene was performed with SNPAlyze 5.1. Relations between the morphine maintenance dose and morphine-induced adverse reactions were evaluated with the use of Spearman's rank correlation coefficient. The Fisher's exact test were employed to analyze the association of *UGT2B7*, *ABCB1*, and *OPRM1* diplotypes or genotypes with morphine-related adverse events as graded by NCI-CTCAE, ver. 3.0 (grade 0 versus other) (JMP version 6 software, SAS Institute, Inc., Cary, NC, USA). A P -value of less than 0.05 was considered to indicate a statistically significant difference.

Results

Patient characteristics and morphine-induced adverse reactions

A total of 32 Japanese patients with cancer who received controlled-release morphine sulfate were enrolled in this study from July 2006 through February 2007. The patient characteristics are summarized in Table 1. The most frequent tumor was breast cancer, followed by colorectal and pancreatic cancers. Most patients (29/32) had metastases to various organ(s). Renal function evaluated on the basis of the serum creatinine level was normal in all patients.

Table 1 Patient characteristics

Characteristics	Values	Number of patients
Age (years) ^a	64.5 (38–77)	32
Sex (male/female)		15/17
Serum creatinine (mg/dl) ^a	0.7 (0.5–1.2)	32
Total bilirubin (mg/dl) ^a	0.4 (0.2–14.4)	32
Tumor type		
Breast		8
Colorectal		7
Pancreas		4
Stomach		3
Esophagus		3
Others		7
Maintenance dose (mg/day)	20/30/40/60/80	21/3/3/4/1
Metastasis	Yes/no	29/3

^a Values are expressed as medians, with ranges in parentheses

Hepatic function estimated on the basis of the total bilirubin level was normal in all but one patient, who had a value of 14.4 mg/dl. Morphine-induced adverse reactions are shown in Table 2. There was no relation between the maintenance dose of morphine and the respective morphine-induced adverse reactions (Spearman's rank correlation coefficient).

Genotype and allele frequencies of polymorphisms in *UGT2B7*, *ABCB1*, and *OPRM1* genes

The genotype and allele frequencies of polymorphisms in the *UGT2B7*, *ABCB1*, and *OPRM1* genes are shown in Table 3. Allele frequencies of polymorphisms in the *UGT2B7* and *ABCB1* genes were roughly equal to those previously reported [7, 11]. The genotype and allele frequencies of 118A > G in the *OPRM1* gene were consistent with the HapMap data reported for Japanese (http://www.ncbi.nlm.nih.gov/SNP/snp_ref.cgi?rs=1799971). All polymorphisms were in Hardy–Weinberg equilibrium ($P > 0.05$). We found that 3435C > T in the *ABCB1* gene was strongly linked to 2677G > T ($r^2 = 0.711$ and $D' = 0.927$), but not to 1236C > T, although Sai et al. [17] demonstrated linkage among 1236C > T, 2677G > T, and 3435C > T.

UGT2B7, *ABCB1*, and *OPRM1* genotypes and morphine-induced adverse reactions

The *UGT2B7**2 genotype was significantly associated with the frequency of nausea (grades 1–3; $P = 0.023$; Fig. 1). The frequency of nausea was higher in patients without *UGT2B7**2 allele than others. However, the systemic oral clearance of morphine did not differ significantly between the two groups of genotype, without *UGT2B7**2 and at least one *UGT2B7**2 allele. The frequency of other adverse reactions were also slightly higher in patients without *UGT2B7**2 than in those with at least one *UGT2B7**2 allele. A71S mutation was not related to any type of morphine-induced adverse events or to morphine clearance.

The genotype at 1236 in *ABCB1* gene was associated with the frequency of fatigue (grades 1–3; $P = 0.012$;

Table 2 Morphine-induced adverse reactions

Adverse reactions	Grade	Numbers of patients
Constipation	0/1/2/3	15/12/4/1
Nausea	0/1/2/3	21/7/3/1
Vomiting	0/1/2/3	25/3/1/1
Drowsiness/confusion	0/1/2/3	22/1/9/0
Fatigue	0/1/2/3	18/7/6/1

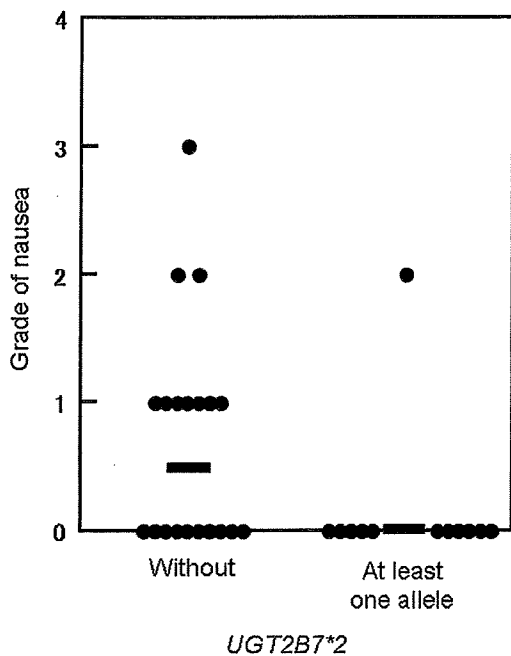


Fig. 1 *UGT2B7*2* genotype and morphine-induced nausea. Bars indicate medians

Fig. 2). The frequency of fatigue in patients with the T/T genotype at 1236 was significantly lower than that with other genotypes. The frequency of fatigue (grades 1–3) was also significantly lower in patients with TT/TT diplotype at 2677 and 3435 in *ABCB1* gene than in other patients ($P = 0.011$; Fig. 2). Morphine oral clearance was slightly but not significantly higher in patients with T/T genotype at 1236 or TT/TT diplotype at 2677 and 3435 than in other patients ($P = 0.103$ and 0.116 , Mann–Whitney *U*-test). The diplotype at 2677 and 3435 in *ABCB1* was associated with the frequency of vomiting (grades 1–3; $P = 0.011$; Fig. 3). No patient without GC allele at 2677 and 3435 suffered from vomiting. The frequency of nausea (grades 1–3) in patients without GC allele at 2677 and 3435 in *ABCB1* was tended to be lower than others ($P = 0.061$). The oral clearance of morphine, M6G, and M3G did not differ significantly between these groups.

Morphine-induced adverse reactions were not associated with the polymorphism of 118A > G in the *OPRM1* gene.

The maintenance dose of morphine did not differ significantly between any two groups divided according to genotypes or diplotype for any of the adverse reactions described above.

Discussion

Our study showed that the grade of morphine-related adverse reactions was associated with genetic polymorphisms in genes

Table 3 Genotype and allele frequencies of polymorphisms in the *UGT2B7*, *ABCB1*, and *OPRM1* genes

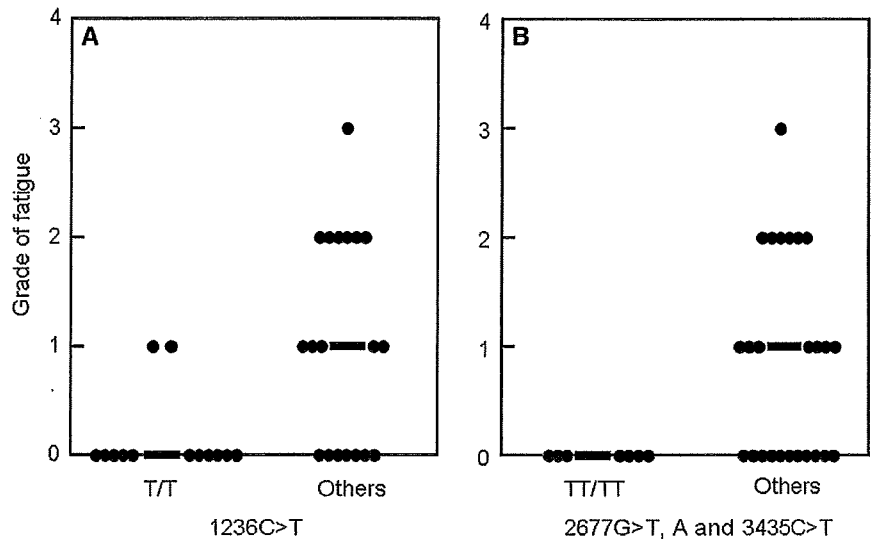
Polymorphism	Genotype	Number (frequency)	Allele Frequency (frequency)
<i>UGT2B7</i> -327G > A	G/G	17 (0.53)	G 0.70
	G/A	11 (0.34)	A 0.30
	A/A	4 (0.13)	
211G > T	G/G	29 (0.91)	G 0.95
	G/T	3 (0.09)	T 0.05
	T/T	0 (0)	
802C/T	C/C	20 (0.62)	C 0.75
	C/T	8 (0.25)	T 0.25
	T/T	4 (0.13)	
<i>ABCB1</i> 1236C > T	C/C	5 (0.16)	C 0.38
	C/T	14 (0.43)	T 0.62
	T/T	13 (0.41)	
2677G > T, A	G/G	6 (0.19)	G 0.39
	G/T	9 (0.28)	T 0.45
	G/A	4 (0.13)	A 0.16
	T/A	4 (0.13)	
	T/T	8 (0.24)	
3435C > T	C/C	7 (0.22)	C 0.5
	C/T	18 (0.56)	T 0.5
	T/T	7 (0.22)	
<i>OPRM1</i> 118A > G	A/A	7 (0.22)	A 0.48
	A/G	17 (0.53)	G 0.52
	G/G	8 (0.25)	

that encode factors related to morphine pharmacokinetics and pharmacodynamics, including *UGT2B7*, *ABCB1*, and *OPRM1*.

The frequency of nausea was higher in patients without *UGT2B7*2* allele than others (Fig. 1); the systemic oral clearance of morphine did not differ significantly between the two groups. Coffman et al. [18] have demonstrated that *UGT2B7.2* is capable of catalyzing morphine to inactive M3G more efficiently than to active M6G. Therefore, morphine might be detoxified more rapidly in patients with *UGT2B7*2* than in other patients, supporting our results that the incidence of morphine-induced adverse events was lower in patients with *UGT2B7*2*.

In our study, the T/T genotype at 1236 or TT/TT diplotype at 2677 and 3435 in *ABCB1* was associated with significantly lower frequency of fatigue (Fig. 2). This difference might be attributed to lower systemic exposure to morphine in patients homozygous for T allele at 1236 or TT/TT diplotype at 2677 and 3435. This notion is supported by the fact that morphine oral clearance in patients

Fig. 2 *ABCB1* genotype or diplotype and morphine-related fatigue **a** 1236C > T, **b** 2677C > T, A and 3435C > T. Bars represent medians



with T/T genotype at 1236 or TT/TT diplotype at 2677 and 3435 tended to be higher than that in other patients. However, Meineke et al. [19] showed that the TT genotype of 3435C > T is associated with lower *ABCB1* expression. To date, the functional effects of 1236C > T, 2677G > T, A, and 3435C > T in the *ABCB1* gene on the pharmacokinetics, efficacy, and adverse events of drugs remain controversial [20–32]. Further studies are necessary to elucidate the roles of these polymorphisms on the functions of *ABCB1*.

The frequency of vomiting was significantly higher in patients with one GC allele at 2677 and 3435 than in other patients (Fig. 3). In contrast, Coulbaut et al. [33] demonstrated that the GC/GC diplotype at 2677 and 3435 in the *ABCB1* gene was significantly associated with lower incidences of morphine-related nausea and vomiting as evaluated by the use of ondansetron. The results of these studies do not agree with our findings. One reason for the discrepancy may be the difference in the administration route of morphine. In our study, morphine was administered orally, whereas in the study by Coulbaut et al. [33], morphine was administered intravenously to control postoperative pain. Since orally administered morphine is subject to the actions of *ABCB1* expressed in the small intestine, the effects of polymorphisms in the *ABCB1* gene on pharmacokinetics might differ between intravenously and orally administered morphine.

Although Campa et al. [12] have shown that pain-relief variability in patients with cancer is significantly associated with 3435C > T in the *ABCB1* gene, they have not found any relations between morphine-induced adverse events and *ABCB1* polymorphisms, which was inconsistent with our present results.

Morphine-induced adverse reactions were not associated with the polymorphism of 118A > G in the *OPRM1* gene. As reported previously, cancer patients homozygous for the

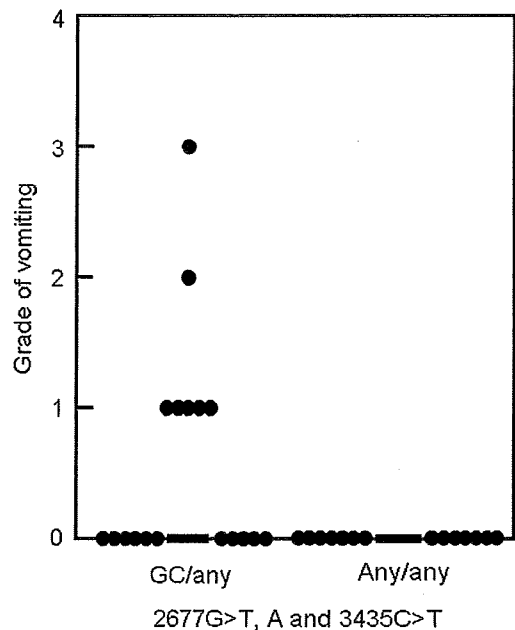


Fig. 3 *ABCB1* diplotype and morphine-induced vomiting. Bars represent medians

G allele were found to be poor responders to morphine [12] and to require higher doses of morphine to relieve pain [16]. These findings suggest that morphine-related adverse reactions are likely to occur in patients with G allele at 118, given that the mechanism of morphine-induced adverse events involves *OPRM1*. However, our results do not support this notion. Further analysis is necessary to confirm whether morphine-induced fatigue is directly related to the function of *OPRM1*.

It has been reported that V158M in catechol-*O*-methyltransferase (COMT) is associated with the response of morphine and further with morphine dose requirement [34]. We

are now investigating the association of morphine-related adverse events with polymorphisms in *COMT*, together with polymorphisms in *UGT2B7*, *ABCB1*, and *OPRM1* which we have not yet examined.

Large prospective studies are needed to determine whether genetic testing for *UGT2B7*, *ABCB1*, and *OPRM1* helps to predict the risk of morphine-induced adverse reactions and to elucidate the detailed mechanisms of morphine-related adverse events, taking into account medical aspects as well as cost effectiveness.

Acknowledgments This study was supported in part by a Grant-in-Aid for Scientific Research (C) (19590542) from the Japan Society for the Promotion of Science to K.F., a grant from the Japan Research Foundation for Clinical Pharmacology to K.F., Grant-in-Aid for Development of New Technology from The Promotion to Y.O. and Mutual Aid Corporation for Private Schools of Japan to Y.O. We thank A. Spareboom (St. Jude Children's Research Hospital) for kind review of our manuscript, Y. Yatsuka and T. Hirata for their technical assistance.

Conflict of interest statement None.

References

- Evans WE, Relling MV (1999) Pharmacogenomics: translating functional genomics into rational therapeutics. *Science* 286:487–491
- Evans WE, McLeod HL (2003) Pharmacogenomics—drug disposition, drug targets, and side effects. *N Engl J Med* 348:538–549
- Evans WE, Relling MV (2004) Moving towards individualized medicine with pharmacogenomics. *Nature* 429:464–468
- Huang RS, Ratain MJ (2009) Pharmacogenetics and pharmacogenomics of anticancer agents. *CA Cancer J Clin* 59:42–55
- Coffman BL, Rios GR, King CD et al (1997) Human UGT2B7 catalyzes morphine glucuronidation. *Drug Metab Dispos* 25:1–4
- Christrup LL (1997) Morphine metabolites. *Acta Anaesthesiol Scand* 41:116–122
- Hirota T, Ieiri I, Takane H et al (2003) Sequence variability and candidate gene analysis in two cancer patients with complex clinical outcomes during morphine therapy. *Drug Metab Dispos* 31:677–680
- Duguay Y, Báár C, Skorpen F et al (2004) A novel functional polymorphism in the uridine diphosphate-glucuronosyltransferase 2B7 promoter with significant impact on promoter activity. *Clin Pharmacol Ther* 75:223–233
- Somogyi AA, Barratt DT, Coller JK (2007) Pharmacogenetics of opioids. *Clin Pharmacol Ther* 81:429–444
- Wandel C, Kim R, Wood M et al (2002) Interaction of morphine, fentanyl, sufentanil, alfentanil, and loperamide with the efflux drug transporter P-glycoprotein. *Anesthesiology* 96:913–920
- Sai K, Itoda M, Saito Y et al (2006) Genetic variations and haplotype structures of the *ABCB1* gene in a Japanese population: an expanded haplotype block covering the distal promoter region, and associated ethnic differences. *Ann Hum Genet* 70:605–622
- Campa D, Gioia A, Tomei A et al (2008) Association of *ABCB1*/*MDR1* and *OPRM1* gene polymorphisms with morphine pain relief. *Clin Pharmacol Ther* 83:559–566
- LaForge KS, Yuferov V, Kreek MJ (2000) Opioid receptor and peptide gene polymorphisms: potential implications for addictions. *Eur J Pharmacol* 410:249–268
- Hoehe MR, Köpke K, Wendel B (2000) Sequence variability and candidate gene analysis in complex disease: association of mu opioid receptor gene variation with substance dependence. *Hum Mol Genet* 9:2895–2908
- Zhang Y, Wang D, Johnson AD et al (2005) Allelic expression imbalance of human mu opioid receptor (*OPRM1*) caused by variant A118G. *J Biol Chem* 280:32618–32624
- Klepstad P, Rakvåg TT, Kaasa S et al (2004) The 118A > G polymorphism in the human mu-opioid receptor gene may increase morphine requirements in patients with pain caused by malignant disease. *Acta Anaesthesiol Scand* 48:1232–1239
- Sai K, Kaniwa N, Itoda M et al (2003) Haplotype analysis of *ABCB1*/*MDR1* blocks in a Japanese population reveals genotype-dependent renal clearance of irinotecan. *Pharmacogenetics* 13:741–757
- Coffman BL, King CD, Rios GR et al (1998) The glucuronidation of opioids, other xenobiotics, and androgens by human UGT2B7Y(268) and UGT2B7H(268). *Drug Metab Dispos* 26:73–77
- Meineke I, Freudenthaler S, Hofmann U et al (2002) Pharmacokinetic modelling of morphine, morphine-3-glucuronide and morphine-6-glucuronide in plasma and cerebrospinal fluid of neurosurgical patients after short-term infusion of morphine. *Br J Clin Pharmacol* 54:592–603
- Kim RB, Leake BF, Choo EF et al (2001) Identification of functionally variant *MDR1* alleles among European Americans and African Americans. *Clin Pharmacol Ther* 70:189–199
- Hoffmeyer S, Burk O, von Richter O et al (2000) Functional polymorphisms of the human multidrug-resistance gene: multiple sequence variations and correlation of one allele with P-glycoprotein expression and activity in vivo. *Proc Natl Acad Sci USA* 97:3473–3478
- Fellay J, Marzolini C, Meaden ER et al (2002) Response to antiretroviral treatment in HIV-1-infected individuals with allelic variants of the multidrug resistance transporter 1: a pharmacogenetics study. *Lancet* 359:30–36
- Nasi M, Borghi V, Pinti M et al (2003) *MDR1* C3435T genetic polymorphism does not influence the response to antiretroviral therapy in drug-naïve HIV-positive patients. *AIDS* 17:1696–1698
- Saitoh A, Singh KK, Powell CA et al (2005) An *MDR1*-3435 variant is associated with higher plasma nelfinavir levels and more rapid virologic response in HIV-1 infected children. *AIDS* 19:371–380
- Verstuyft C, Marcellin F, Morand-Joubert L et al (2005) Absence of association between *MDR1* genetic polymorphisms, indinavir pharmacokinetics and response to highly active antiretroviral therapy. *AIDS* 19:2127–2131
- Haas DW, Smeaton LM, Shafer RW et al (2005) Pharmacogenetics of long-term responses to antiretroviral regimens containing Efavirenz and/or Nelfinavir: an Adult Aids Clinical Trials Group Study. *J Infect Dis* 192:1931–1942
- Kajinami K, Brousseau ME, Ordovas JM et al (2004) Polymorphisms in the multidrug resistance-1 (*MDR1*) gene influence the response to atorvastatin treatment in a gender-specific manner. *Am J Cardiol* 93:1046–1050
- Siddiqui A, Kerb R, Weale ME et al (2003) Association of multidrug resistance in epilepsy with a polymorphism in the drug-transporter gene *ABCB1*. *N Engl J Med* 348:1442–1448
- Zheng HX, Webber SA, Zeevi A et al (2004) The impact of pharmacogenomic factors on steroid dependency in pediatric heart transplant patients using logistic regression analysis. *Pediatr Transplant* 8:551–557
- Yi SY, Hong KS, Lim HS et al (2004) A variant 2677A allele of the *MDR1* gene affects fexofenadine disposition. *Clin Pharmacol Ther* 76:418–427
- Morita N, Yasumori T, Nakayama K (2003) Human *MDR1* polymorphism: G2677T/A and C3435T have no effect on *MDR1* transport activities. *Biochem Pharmacol* 65:1843–1852

32. Kimchi-Sarfaty C, Gribar JJ, Gottesman MM (2002) Functional characterization of coding polymorphisms in the human MDR1 gene using a vaccinia virus expression system. *Mol Pharmacol* 62:1–6
33. Coulbault L, Beaussier M, Verstuyft C et al (2006) Environmental and genetic factors associated with morphine response in the post-operative period. *Clin Pharmacol Ther* 79:316–324
34. Reyes-Gibby CC, Shete S, Rakvåg T et al (2007) Exploring joint effects of genes and the clinical efficacy of morphine for cancer pain: OPRM1 and COMT gene. *Pain* 130:25–30

Differential Requirement for Nucleostemin in Embryonic Stem Cell and Neural Stem Cell Viability

JUN NOMURA,^a MASAYOSHI MARUYAMA,^a MIYUKI KATANO,^a HIDEMASA KATO,^a JIAXING ZHANG,^a SHINJI MASUI,^b YOSUKE MIZUNO,^c YASUSHI OKAZAKI,^c MASAZUMI NISHIMOTO,^a AKIHIKO OKUDA^{a,d}

^aDivision of Developmental Biology and ^cDivision of Functional Genomics and Systems Medicine, Research Center for Genomic Medicine, Saitama Medical University, Yamane Hidaka, Saitama, Japan; ^bDivision of Molecular Biology and Cell Engineering, Department of Regenerative Medicine, Research Institute, International Medical Center of Japan, Shinjuku-ku, Tokyo, Japan; ^dCore Research for Evolutional Science and Technology (CREST), Japan Science and Technology Agency, Kawaguchi, Saitama, Japan

Key Words. Apoptosis • Embryonic stem cells • Neural stem cell • p53 • Pluripotent stem cells • Proliferation • Self-renewal

ABSTRACT

Stem cells have the remarkable ability to self-renew and to generate multiple cell types. Nucleostemin is one of proteins that are enriched in many types of stem cells. Targeted deletion of nucleostemin in the mouse results in developmental arrest at the implantation stage, indicating that nucleostemin is crucial for early embryogenesis. However, the molecular basis of nucleostemin function in early mouse embryos remains largely unknown, and the role of nucleostemin in tissue stem cells has not been examined by gene targeting analyses due to the early embryonic lethality of nucleostemin null animals. To address these questions, we generated inducible nucleostemin null embryonic

stem (ES) cells in which both alleles of nucleostemin are disrupted, but nucleostemin cDNA under the control of a tetracycline-responsive transcriptional activator is introduced into the *Rosa26* locus. We show that loss of nucleostemin results in reduced cell proliferation and increased apoptosis in both ES cells and ES cell-derived neural stem/progenitor cells. The reduction in cell viability is much more profound in ES cells than in neural stem/progenitor cells, an effect that is mediated at least in part by increased induction and accumulation of p53 and/or activated caspase-3 in ES cells than in neural stem/progenitor cells. *STEM CELLS* 2009;27:1066–1076

Disclosure of potential conflicts of interest is found at the end of this article.

INTRODUCTION

Stem cells possess two remarkable abilities: to self-renew and to generate all the differentiated cell types in the tissue in which they reside [1]. Gene expression profiling data from many tissues have led to the identification of genes that are expressed in many types of stem cells, some of which are required for self-renewal [2–5]. *Sox2* [6–8], *Zfx* [9], *Jam-B* [10], and nucleostemin [11] are examples of genes expressed in a variety of stem cells. Nucleostemin is a nucleolar GTP-binding protein that regulates cell cycle progression and is required for early embryogenesis, with deletion of the gene resulting in embryonic lethality at around 3.5 days postcoitum (d.p.c.) [12, 13]. As nucleostemin is known to interact with the tumor suppressor protein p53, this raises the possibility that the embryonic lethality in nucleostemin mutants might be caused by loss of nucleostemin-mediated p53 repression. However, as loss of p53 fails to rescue the nucleostemin phenotype, it is unlikely that p53 alone mediates nucleostemin function in cell proliferation [12]. Nucleostemin protein is detected at high levels in the nucleus, particularly the nucleolus,

of stem cells, but is lost abruptly when the cells are induced to differentiate [11, 14]. Thus, it is generally assumed that nucleostemin plays an important role in stem cell proliferation. However, with the exception of a few studies using stromal stem cells from adult human bone marrow [15], most studies investigating nucleostemin function have been performed using nonstem cells, such as U2OS osteosarcoma cells [16–18]. The role of nucleostemin in stem cells is therefore still unclear.

Here, we demonstrate that nucleostemin plays a crucial role in controlling the cell proliferation rate and apoptosis level in embryonic stem (ES) cells and ES cells-derived neural stem/progenitor cells. We generated nucleostemin knock-out ES cells carrying a tetracycline-regulatable nucleostemin expression cassette (*nucleostemin*^{-/-}; *Rosa26-NS*). In accordance with previous data demonstrating that Oct-3/4 is strongly expressed in inner cell mass cells of nucleostemin null blastocysts [12], our data indicate that nucleostemin is not involved in maintaining pluripotency of ES cells. Our data also demonstrate that nucleostemin is not required for preserving multipotency of neural stem/progenitor cells. Interestingly, loss of nucleostemin shows a stronger effect in ES cells than in

Author contributions: J.N.: data analysis and interpretation, manuscript writing; M.M., J.Z., M.K., and H.K.: data analysis and interpretation; S.M.: provision of study materials, data analysis and interpretation; Y.M. and Y.O.: data analysis and interpretation (DNA microarray analyses); M.N.: data analysis and interpretation; A.O.: conception and design, manuscript writing, administrative support.

Correspondence: Akihiko Okuda, M.D., Ph.D., 1397-1 Yamane, Hidaka, Saitama, Japan. Telephone: 81-42-985-7268; Fax: 81-42-985-7264; e-mail: akiokuda@saitama-med.ac.jp Received September 4, 2008; accepted for publication February 6, 2009; first published online in *STEM CELLS EXPRESS* February 20, 2009. © AlphaMed Press 1066-5099/2009/\$30.00/0 doi: 10.1002/stem.44

STEM CELLS 2009;27:1066–1076 www.StemCells.com

neural stem cells. Nucleostemin null neural stem cells can propagate, albeit slowly, whereas no viable null ES cells can be maintained during a long culture period. Our data suggest that this difference is at least partly due to the differences in magnitude of p53 and/or caspase-3 activation between these two different stem cell types.

MATERIALS AND METHODS

Plasmid Construction

To generate a targeting vector for the nucleostemin locus, a XhoI/AscI 4.9 kb 5' flanking region including the first exon was used for the upstream homologous region, whereas a SalI/EcoRI 2.7 kb DNA fragment carrying the regions from exon 12 to the end of the gene was used for the downstream homologous region. These two DNA fragments were subcloned into the pBR322-base plasmid and the *IRES- β -geo* reporter gene [19] was inserted between them. For Tet-off expression of the nucleostemin gene, nucleostemin cDNA was subcloned into the XhoI/NotI sites of the exchange vector pZhCSfi, together with the polyA signal from bovine growth hormone gene [20]. The Cre recombinase expression vector pCAGGS-Cre has been described elsewhere [21]. For construction of the Flag-Bcl-2 expression vector, the Flag sequence was placed in front of the entire coding region of Bcl-2 and the resultant Flag-Bcl-2 DNA fragment was subcloned into the EcoRI site of pCAGIPuro so that a Flag-Bcl-2-IRES-puromycin fusion RNA transcript is generated in cells [22]. Construction of the luciferase reporter plasmid with multimerized p53 binding sites was done by subcloning oligonucleotides containing four copies of the p53 binding site in front of the SV40 minimal early promoter of the pGL3-Promoter vector (Promega, Madison, WI, <http://www.promega.com>).

ES Cell Culture and Generation of Nucleostemin Knockout ES Cells Carrying a Tetracycline-Regulatable Nucleostemin Expression Cassette

ERBTcH3 ES cells [20] were maintained without feeder cells. These ES cells were cultured with a standard medium containing fetal bovine serum and leukemia inhibitory factor, as described before [23]. To generate nucleostemin null ES cells, targeting vector of nucleostemin was introduced into ES cells by electroporation for homologous recombination, according to Thomas and Capecchi [24]. After selection in G418, heterozygous nucleostemin ES cell clones were identified by Southern blot analysis. Introduction of nucleostemin cDNA and the Tet-off system was performed as described previously [20]. The cells were then cultured at high G418 concentration (10 mg/ml) to eliminate the remaining wild-type nucleostemin locus.

Genotyping

Genomic DNA was extracted from ES cells and used for genotyping by Southern blotting or polymerase chain reaction (PCR). Southern blot analysis was done as described previously [10] using 5' and 3' flanking regions of nucleostemin gene. For genotyping by PCR, three different primers were used to amplify a portion of wild-type nucleostemin gene and a boundary region of the *β -geo* reporter gene. The sequences of these primers are as follows:

5'-GAGCATGCAGATTGTCCCTTTA-3'
5'-CATAATCAGCCATATCACATCTGTAGAGGT-3'
5'-CTTGTATGCTGTGTGCATTA-3'.

RNA and Protein Analysis

For reverse transcription polymerase chain reaction (RT-PCR) analysis, an oligo-dT primed reverse transcription was carried out

using 1 μ g of total RNA, and 1/40 of the single strand cDNA products was used for each PCR reaction. Before performing PCR with the RT products, the number of reaction cycles was determined to achieve semiquantitative conditions with control DNA for each primer set. For western blot analysis, extract treated with sample buffer was used to detect specific protein by chemiluminescence, as described previously [25].

Immunocytochemistry

Indirect immunocytochemistry was carried out as previously described [26] with cells that had been cultured on coverslips coated with poly-D-lysine and laminin. For 5-Bromo-2'-deoxyuridine (BrdU) labeling experiments, cells were treated with 10 μ g/ml BrdU for 30 minutes. Subsequently, cells were incubated with 4 N HCl for 10 minutes, then rinsed with 0.1 M borate buffer (pH 8.5) for 30 minutes before immunostaining.

Antibodies

Generation of anti-Oct-3/4 and undifferentiated embryonic cell transcription factor 1 (UTF1) antibodies were described previously [25, 27]. The following commercially available antibodies were used in this study: anti-nucleostemin (AB5691; CHEMICON), anti-Fibrillarin (H-140; Santa Cruz Biotechnology, Santa Cruz, CA, <http://www.scbt.com>), anti-Caspase-3 (9662; Cell Signaling Technology, Beverly, MA, <http://www.cellsignal.com>), anti-p53 (NCL-p53-CM5p; Novocastra, Newcastle upon Tyne, U.K., <http://www.novocastra.co.uk>), anti- β -actin (C-4; Santa Cruz Biotechnology), anti-Nestin (clone RAT401; BD PharMingen, San Diego, http://wwwbdbiosciences.com/index_us.shtml), anti-microtubule-associated protein 2 (clone HM-2; Sigma), anti-gial fibrillary acidic protein (clone GA5; Sigma), and anti-BrdU (clone BMC9318; Roche, Basel, Switzerland, <http://www.roche-applied-science.com>).

Transfection and Luciferase Assay

For the luciferase assay, ES cells were transfected in 24-well dishes with the luciferase gene reporter plasmid bearing multimerized p53 binding sites (0.8 μ g) and internal control pRL/CMV vector (Promega; 0.08 μ g) using lipofectamine 2000. Twenty-four hours post-transfection, transcription levels were determined according to the manufacturer's instructions. To obtain stable transformants of Bcl2, *nucleostemin*^{-/-}; *Rosa26-NS* ES cells were transfected with plasmid carrying a *Flag-tagged Bcl-2-IRES-puromycin* expression cassette under the control of *β -actin* promoter by lipofection as above-mentioned and then selected with puromycin. Among 50 independent stable transformants, one clone showing high and stable Flag-Bcl2 expression was selected by western blot analysis.

Flow Cytometry

Nucleostemin^{-/-}; *Rosa26-NS* ES cells were either treated with doxycycline for 4 days or left untreated. Cells were then recovered and were stained with Alexa 488 Fluor dye-conjugated annexin V and propidium iodide (PI) and were subjected to flow cytometry (FACS Calibur, BD Bioscience) using CellQuest Pro software. A minimum of 10,000 cells were used for each analysis.

DNA Microarray Analysis

RNA was prepared from doxycycline-treated or -untreated *nucleostemin*^{-/-}; *Rosa26-NS* ES cells and were used for generating cRNA using one-cycle target labeling and control reagents from Affymetrix (Santa Clara, CA, <http://www.affymetrix.com>). Fifteen microgram of cRNA was cleaved into 35–200 base fragments according to the manufacturer's instructions (Affymetrix). The fragmented cRNA was mixed with hybridization solution and hybridized to Mouse Genome 430A 2.0 arrays. Hybridized arrays were scanned and analyzed by GeneChip Scanner 3000

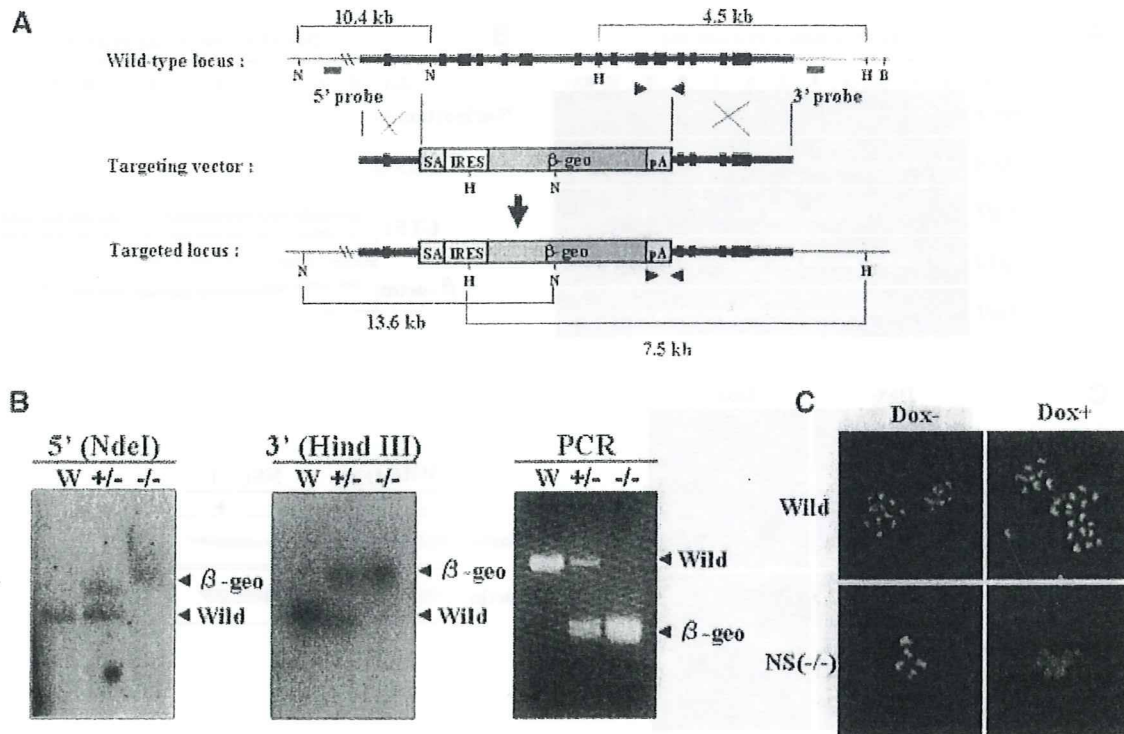


Figure 1. Generation of nucleostemin knockout embryonic stem (ES) cells carrying a doxycycline-regulatable nucleostemin expression unit. (A): Schematic diagrams of nucleostemin targeting vector and wild-type and *IRES- β -geo* knock-in alleles of the nucleostemin gene. The 5' and 3' probes were located outside the homology arms of the targeting vector. Solid triangle indicates primer for genotyping PCR. Restriction enzymes indicated are as follows: N, NdeI, H, HindIII, B, BamHI. (B): Genotyping of wild-type and *IRES- β -geo* knock-in alleles of the nucleostemin gene by Southern blot and PCR analyses. NdeI- and HindIII-digested genomic DNA from ES cells was hybridized with 5' and 3' probe, respectively. For PCR-based genotyping, undigested genomic DNA was used to detect the wild-type and knock-in alleles using three different primers, as described in the "Materials and Methods" section. (C): No nucleostemin expression in *nucleostemin*^{-/-}; *Rosa26-NS* ES cells cultured in the presence of doxycycline. The ERBTcH3 parental ES cells (wild-type) [20] or *nucleostemin*^{-/-}; *Rosa26-NS* ES cells were cultured on coverslips coated with poly-D-lysine and laminin for 4 days either with or without doxycycline. After fixation, cells were immunostained with anti-nucleostemin antibody and counterstained with 4',6'-diamidino-2-phenylindole. Abbreviations: DOX, doxycycline; IRES, internal ribosome entry site; NS, nucleostemin; PCR, polymerase chain reaction; SA, splice acceptor site.

and GCOS software. Raw data of DNA microarray analysis are available on request.

Generation of Neural Stem/Progenitor Cells from *Nucleostemin*^{-/-}; *Rosa26-NS* ES Cells

To induce neural lineage commitment, *nucleostemin*^{-/-}; *Rosa26-NS* ES cells were cultured in the absence of doxycycline under adherent monolayer differentiation conditions, as previously described [28]. On day 7, conversion of a heterogeneous cell population obtained by neural induction to a pure population of neural stem/progenitor cells was performed as previously described [29]. Cells were passaged several times to obtain a cell population uniformly positive for nestin expression.

RESULTS

Generation of Nucleostemin Null ES Cells

To assess the requirement for nucleostemin in ES cells and ES cell-derived neural stem/progenitor cells, we set out to disrupt both alleles of nucleostemin in ERBTcH3 ES cells [20]. We first prepared a targeting vector for the nucleostemin locus carrying an *IRES- β -geo* reporter gene. The vector is designed to replace 10 exons (from exon 2 to exon 11), which

cover most of the basic domains involved in nucleolar targeting/p53 interaction and all of the GTP-binding domain involved in partitioning the protein between the nucleolus and the nucleoplasm (Fig. 1A). After linearization, the vector was introduced into ES cells by electroporation. Southern blot analysis revealed that the targeting vector disrupted the gene correctly in 3 of 480 independent G418-resistant clones (Fig. 1B). Subsequently, nucleostemin cDNA was introduced into the *Rosa26* locus, which was altered to contain a tetracycline-responsive transcriptional activator and to permit any cDNA to be introduced using a recombination-mediated cassette exchange reaction (see supporting information Fig. 1 for reference). As a final step, we disrupted the remaining wild-type allele of nucleostemin by culturing *nucleostemin*^{+/-} ES cells under high G418 conditions (10 mg/ml). This high G418 selection was done in the absence of doxycycline to allow expression of exogenous nucleostemin from *Rosa26* locus, and thus preventing cell death coupled to nucleostemin loss. This procedure yielded two independent ES cell clones (*nucleostemin*^{-/-}; *Rosa26-NS*) that grew at a normal rate even in the presence of high G418. Southern blot analysis revealed that the remaining nucleostemin locus was indeed disrupted in these two independent clones (Fig. 1B). Loss of nucleostemin in these cells was also confirmed by PCR (Fig. 1B) and immunostaining of cells cultured in the presence of doxycycline (Fig. 1C).

STEM CELLS

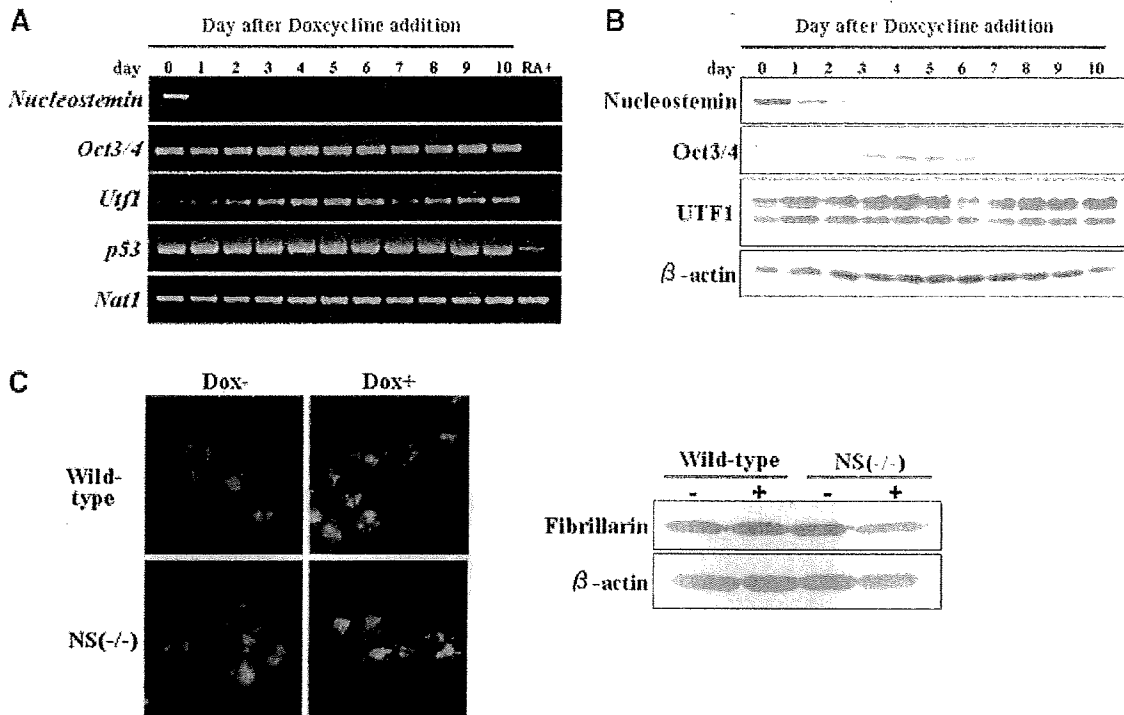


Figure 2. Normal expression of pluripotency genes and integrity of nucleolar structure of embryonic stem (ES) cells in the absence of nucleostemin expression. (A): Semiquantitative reverse transcription polymerase chain reaction analysis of total RNA prepared from *nucleostemin*^{-/-}; *Rosa26-NS* ES cells cultured in the presence of doxycycline on the indicated days. Retinoic acid-treated ERBTcH3 ES cells were used as reference for differentiated cells. RNA level of the ubiquitously expressed gene *Nat1* [30] was used as an internal control. (B): Western blot analysis of extracts from *nucleostemin*^{-/-}; *Rosa26-NS* ES cells cultured with doxycycline on the indicated days. Upper and lower bands obtained with anti-UTF1 antibody correspond to the entire UTF1 protein (amino acids; 1–339) and a fragment lacking the amino terminus (amino acids; 43–339) [31]. Anti- β -actin antibody was used for western blot analysis to confirm the equivalent amount of protein used for each lane. (C): Normal nucleolar structure in *nucleostemin*^{-/-}; *Rosa26-NS* ES cells. Immunocytochemical and western blot analyses were performed with ERBTcH3 (wild-type) and *nucleostemin*^{-/-}; *Rosa26-NS* [NS (-/-)] ES cells using anti-Fibrillarini antibody. For immunocytochemical analysis, cells were counterstained with 4',6'-diamidino-2-phenylindole. Abbreviations: DOX, doxycycline; NS, nucleostemin; RA, retinoic acid; UTF1, undifferentiated embryonic cell transcription factor 1.

Pluripotent Marker Expression Was Preserved in Nucleostemin Null ES Cells

We first examined whether loss of nucleostemin affects the pluripotent state of ES cells. To this end, we examined the expression of specific markers of pluripotency. As shown in Figure 2A, we confirmed that nucleostemin expression from the *Rosa26* locus was rapidly downregulated upon addition of doxycycline to the culture medium. However, the expression levels of pluripotent markers, such as Oct-3/4 [27, 32] and UTF1 [25], were unaffected at both the RNA (Fig. 2A) and protein (Fig. 2B) levels by the loss of nucleostemin expression. *p53* and *Nat1* were used as controls. We also confirmed the nucleolar integrity of nucleostemin null ES cells by both nucleolar morphology and expression level of the nucleolar protein fibrillarini (Fig. 2C), corroborating results from other groups with embryonic blastocysts [12] and the human osteosarcoma U2OS cell line [16].

Loss of Nucleostemin in ES Cells Results in a Decrease in Cell Proliferation Rate and Increased Apoptosis

Although loss of nucleostemin in ES cells did not affect the pluripotency of ES cells, it did result in the failure of long-term culture. *Nucleostemin*^{-/-}; *Rosa26-NS* ES cells appear to

stop growing within 5 days after addition of doxycycline (Fig. 3A, lower panels), and no viable cells are detectable within 21 days (data not shown). However, cells cultured in the absence of doxycycline grow at the same rate as do parental ERBTcH3 ES cells (Fig. 3A, upper panels) and can be subjected to long-term culture (data not shown). As the Tet-off system can be manipulated in the in vivo by administering doxycycline in the drinking water of mice [33, 34], we also examined the relationship between nucleostemin expression and tumorigenic properties of ES cells. We found that without doxycycline administration, *nucleostemin*^{-/-}; *Rosa26-NS* ES cells were able to produce large tumors when injected subcutaneously into nude mice. However, when doxycycline was administered, these cells did not generate visible tumors (data not shown).

To further characterize the effect of the loss of nucleostemin, we examined cell proliferation and apoptosis in nucleostemin null ES cells. We found that the proliferation rate of nucleostemin null ES cells is reduced compared to wild-type, as demonstrated by BrdU incorporation assays (Fig. 3B). Activated caspase-3 is also detected in nucleostemin null ES cells (Fig. 3C), suggesting that the reduced cell viability of nucleostemin null ES cells is due to elevated levels of apoptosis. When assessed by annexin V staining, we found twice as many apoptotic cells in nucleostemin null ES cells (doxycycline-treated; 19.0% \pm 2.36%) as in untreated ES cells (9.75% \pm 0.35%). Early apoptotic cells

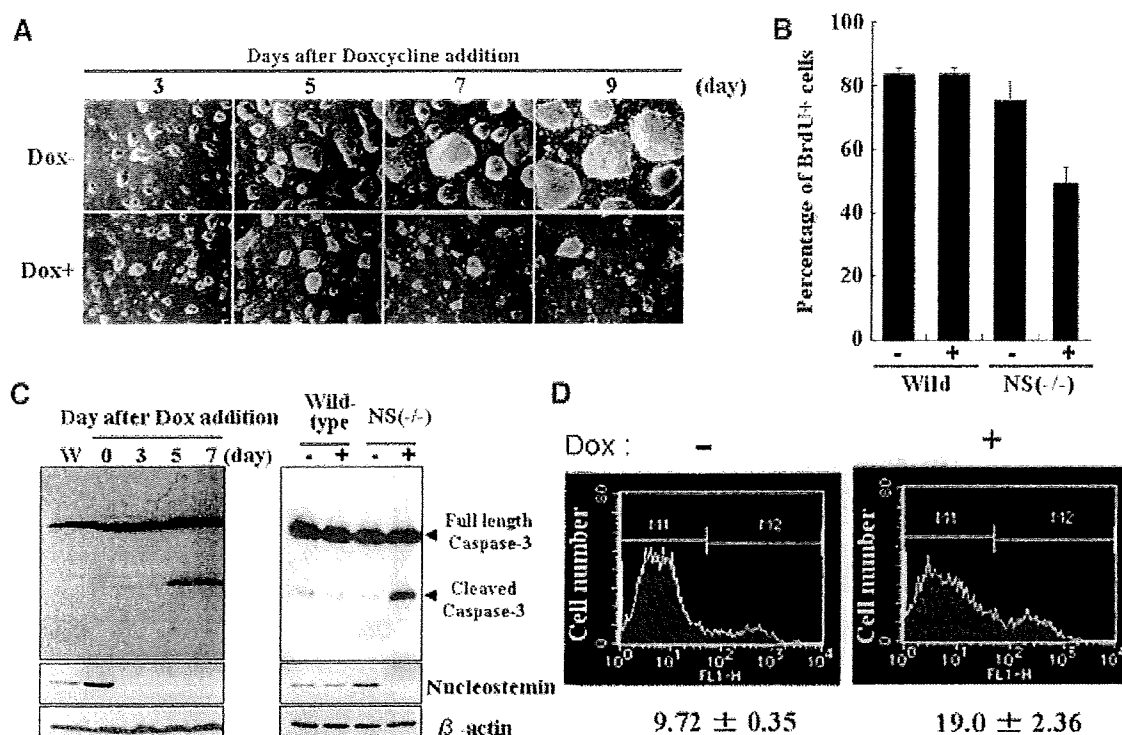


Figure 3. Phenotypes of nucleostemin null embryonic stem (ES) cells. (A): Morphological changes of *nucleostemin*^{-/-}; *Rosa26-NS* ES cells due to the loss of nucleostemin expression. (B): Reduced cell proliferation of nucleostemin null ES cells. ERBTcH3 (wild-type) or *Nucleostemin*^{-/-}; *Rosa26-NS* [NS(-/-)] ES cells cultured in the presence or absence of doxycycline for 4 days were treated with BrdU for 30 minutes. Incorporation of BrdU was determined by immunocytochemistry. For quantification of BrdU labeling, the number of total cells (DAPI positive) and immunoreactive cells in a fixed area (218 \times 162 μ m²) of random area was counted. For each case, three different samples were used to obtain standard deviations. (C): Level of activated caspase-3 is elevated in nucleostemin null ES cells. Cell extracts from doxycycline-treated *nucleostemin*^{-/-}; *Rosa26-NS* ES cells for the indicated days were subjected to western blot analysis using anti-Caspase-3, anti-nucleostemin, or anti- β -actin antibodies (left panel). ERBTcH3 (wild-type) or *nucleostemin*^{-/-}; *Rosa26-NS* [NS(-/-)] ES cells were treated with doxycycline for 4 days or were left untreated. Extracts were then prepared for western blot analysis (right panel). (D): Loss of nucleostemin is accompanied by an elevation of the level of apoptosis in ES cells. Doxycycline-treated (4 days) or untreated *nucleostemin*^{-/-}; *Rosa26-NS* [NS(-/-)] ES cells were stained with Alexa 488 Fluor dye-conjugated annexin V and were subjected to fluorescence-activated cell sorting analyses. Data were obtained from three independent experiments with comparable results. Abbreviations: BrdU, 5-Bromo-2'-deoxyuridine; DOX, doxycycline; FL1-H, fluorescence 1-height; NS, nucleostemin; RA, retinoic acid.

(positive for annexin binding, but negative for PI) also doubled in number as the cells lose nucleostemin (untreated, 2.31% \pm 0.11%; doxycycline-treated, 4.89% \pm 0.51%; data not shown). To reduce the apoptosis level of nucleostemin null ES cells, an expression vector encoding a Flag-tagged version of the anti-apoptotic factor Bcl-2 was stably introduced in the absence of doxycycline, and then cells were treated with doxycycline. We confirmed the expression of Flag-Bcl-2 and the concomitant extinction of activated caspase-3 expression both in the presence and absence of doxycycline (supporting information Fig. 2A). However, we found that Bcl2-overexpressing nucleostemin null ES cells failed to maintain their viability when the cells were cultured at clonal density (2,500 cells per 10-cm dish; supporting information Fig. 2B) or regular density (5 \times 10⁵ per 10-cm dish; data not shown). These results indicate that cell death pathways independent of the activated caspase-3 also operate in nucleostemin null ES cells (for details, see "Discussion" section).

Accumulation of p53 and the Activation of Its Target Genes in Nucleostemin Null ES Cells

As nucleostemin is known to interact with the tumor suppressor protein p53, we examined the levels of p53 mRNA

and protein in nucleostemin null ES cells. Although we did not observe a noticeable increase in the level of p53 mRNA (Fig. 2A), the level of p53 protein is greatly elevated in nucleostemin null ES cells (Fig. 4A). These results indicate that the accumulation of p53 protein in nucleostemin null ES cells is regulated at the post-transcriptional level. As it is known that stability of p53 protein is regulated by proteasome-mediated protein degradation [35, 36], and that nucleostemin either positively or negatively regulates proteasome-dependent protein degradation in U2OS cells, depending on whether it is overexpressed or knocked down [16]. Therefore, we hypothesized that nucleostemin affects the stability of p53 by modulating the efficiency of proteasome-dependent degradation. To examine this possibility, we treated cells with the proteasome inhibitor MG132. While MG132 treatment significantly increases the level of p53 protein in ERBTcH3 cells or in doxycycline-untreated *nucleostemin*^{-/-}; *Rosa26-NS* ES cells, the level of p53 protein in doxycycline-treated nucleostemin null ES cells was not significantly changed by MG132 treatment (Fig. 4B). These results indicate that accumulation of p53 protein in nucleostemin null ES cells is due to inefficient proteasome-dependent degradation of p53.

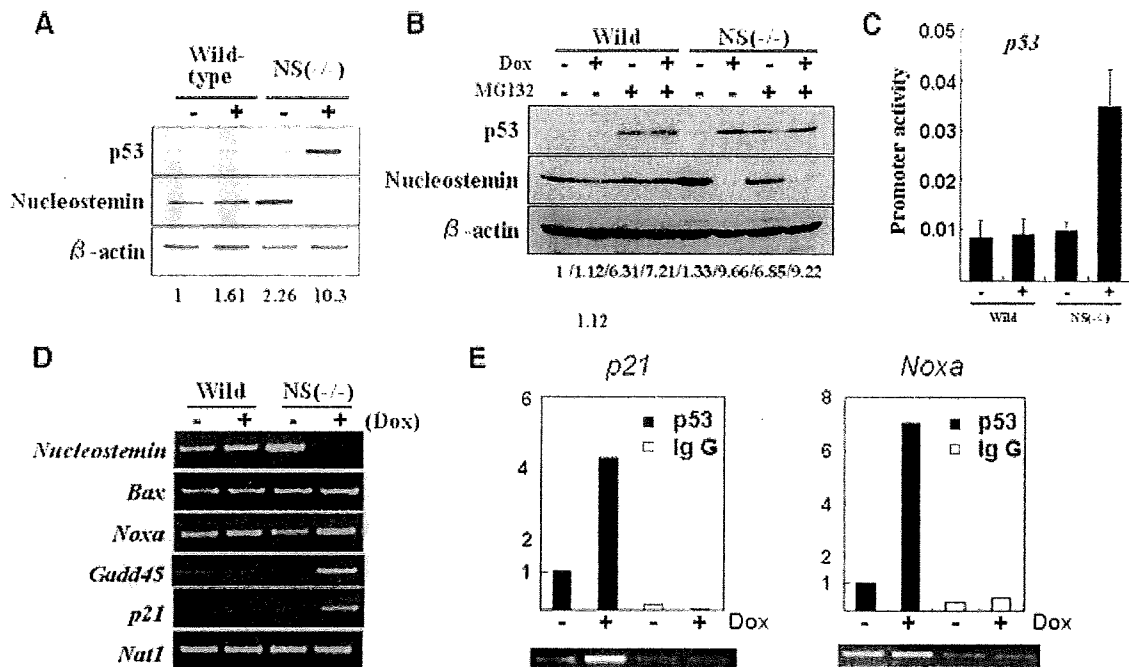


Figure 4. Function of p53 in embryonic stem (ES) cells lacking nucleostemin. (A): Elevation of p53 protein level in nucleostemin null ES cells. Extracts from ERBTcH3 (wild-type) or *nucleostemin*^{-/-}; *Rosa26-NS* [NS(-/-)] ES cells cultured with or without doxycycline for 4 days were subjected to western blot analysis using the indicated antibodies. (B): Accumulation of p53 protein is due to inefficient proteasome-mediated degradation of p53 protein in nucleostemin null ES cells. ERBTcH3 (wild-type) or *nucleostemin*^{-/-}; *Rosa26-NS* [NS(-/-)] ES cells were cultured with or without doxycycline for 4 days. Subsequently, these cells were treated with proteasome inhibitor MG132 (5 μ M) or left untreated for 4 hours. Extracts from these cells were then subjected to western blot analysis using the indicated antibodies. (C): Functional activation of p53 in nucleostemin null ES cells. The luciferase reporter gene carrying multimerized p53 binding sites and the SV40 minimal early promoter was introduced by lipofection together with the internal control pRL/CMV vector into ERBTcH3 (wild-type) or *nucleostemin*^{-/-}; *Rosa26-NS* [NS(-/-)] ES cells pretreated with doxycycline for 4 days or left untreated. Doxycycline-treated and untreated conditions were maintained after lipofection. Forty-eight hours post-transfection, whole cell extracts were prepared and dual-luciferase reporter assays were performed. Activity obtained with luciferase reporter plasmid carrying β -actin regulatory region was arbitrarily set as one. Data were obtained from three independent experiments with comparable results. (D): Elevation of endogenous gene expression levels of some, but not all, putative p53 target genes in nucleostemin null ES cells. Semiquantitative reverse transcription polymerase chain reaction (RT-PCR) was performed with total RNA from ERBTcH3 or *nucleostemin*^{-/-}; *Rosa26-NS* ES cells cultured in the presence or absence of doxycycline. (E): Chromatin immunoprecipitation analyses of p53 downstream genes. Chromatins prepared from doxycycline-treated or untreated *nucleostemin*^{-/-}; *Rosa26-NS* ES cells were immunoprecipitated with anti-p53 antibody or control IgG. The recovered chromatin-DNAs were subjected to semiquantitative RT-PCR and real-time PCR to amplify either p53 binding site-containing regions of *p21* or *Noxa* genes. The amount of DNA recovered with anti-p53 antibody from doxycycline-untreated *nucleostemin*^{-/-}; *Rosa26-NS* ES cells was arbitrarily set to one. Abbreviations: DOX, doxycycline; NS, nucleostemin.

Next, to confirm that the overall activity of p53 is elevated in nucleostemin null ES cells, we performed transient transfection assays with a luciferase reporter gene carrying multiple p53 binding sites and the SV40 minimal early promoter. The reporter activity was elevated in nucleostemin null ES cells (Fig. 4C), indicating that the overall activity of p53 is elevated in nucleostemin null ES cells. We also examined the levels of endogenous expression of putative p53 downstream genes. Although no noticeable increase in *Bax* expression was observed in nucleostemin null ES cells, *Gadd45*, *p21*, and *Noxa* expression levels were increased, albeit only slightly for *Noxa* (Fig. 4D). This lack of *Bax* induction may be due to the fact that unlike in human cells [37], mouse *Bax* expression is not under the control of p53 [38].

Next, to confirm that the elevated levels of gene expression of p53 downstream genes are due to an increase in the efficiency of p53-binding to their promoters, we performed a chromatin immunoprecipitation assay. We immunoprecipitated chromatin from the doxycycline-treated and -untreated *nucleostemin*^{-/-}; *Rosa26-NS* ES cells with anti-p53 antibody or control IgG. We then quantitated the amounts of p53-binding sites present in *p21* and *Noxa* genes by semiquantitative PCR

as well as real time PCR. As shown in Figure 4E, we confirmed that, in both the cases, genomic DNA around p53-binding sites was more efficiently immunoprecipitated in doxycycline-treated nucleostemin null ES cells than in untreated cells. We also obtained a similar result with the p53-binding site present in the third intron of *Gadd45* gene (data not shown).

As the above-mentioned results suggested that decreased cell viability upon loss of nucleostemin may be mediated by p53, we examined the effect of a p53 inhibitor Pifithrin- α [39] on viability of nucleostemin null ES cells. This treatment impaired p53-binding site-dependent transcriptional activation in a dose-dependent manner (Fig. 5A) and elevation of endogenous *Gadd45*, *p21*, and *Noxa* expression levels (data not shown). Consistent with these results, higher concentration of Pifithrin- α (20 μ M) partially rescued nucleostemin null ES cells (Fig. 5B), although cells grew extremely slowly (sizes of colonies shown at day 8 and 16 are about of equivalent sizes to colonies of doxycycline-untreated cells at day 3 and 6, respectively). The rescued cells were alkaline phosphatase-positive, implicating that pluripotency is retained and could be subjected to passage at least three times, although

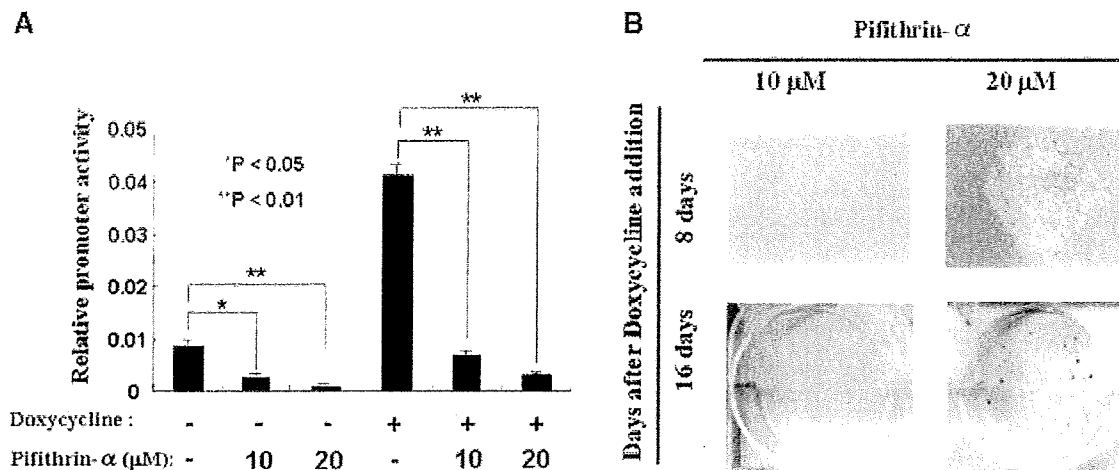


Figure 5. Rescue of nucleostemin null embryonic stem (ES) cells with Pifithrin- α . (A): Inhibition of p53 activity with Pifithrin- α in nucleostemin null ES cells. The luciferase reporter gene carrying multimerized p53-binding sites used in Figure 4C was introduced by lipofection together with the internal control pRL/CMV vector into *nucleostemin*^{-/-}; *Rosa26-NS* [NS(-/-)] ES cells pretreated with doxycycline for 4 days or left untreated. These cells were also pretreated or untreated with Pifithrin- α for 2 days. These conditions were maintained after lipofection. Forty-eight hours post-transfection, whole cell extracts were prepared and dual-luciferase reporter assays were performed. Activity obtained with luciferase reporter plasmid carrying β -actin regulatory region was arbitrarily set as one. Data were obtained from three independent experiments with comparable results. (B): Pifithrin- α partially counteracts the detrimental effect of nucleostemin loss in ES cells. *Nucleostemin*^{-/-}; *Rosa26-NS* [NS(-/-)] ES cells were transferred to 6-well dishes at clonal density (400 cells per well). Doxycycline treatment was started from the next day. After 48 hours post doxycycline addition, Pifithrin- α was added to the indicated concentration. The obtained colonies were observed under microscope and were subjected to Leishman's staining after 8 and 16 days post doxycycline addition, respectively.

substantial cell death occurred during each passage (data not shown). These results support the idea that reduction in cell viability of nucleostemin null cells is at least in part due to the accumulated p53. We will discuss about possibilities which could explain the partial, but not complete, rescue with Pifithrin- α later (see "Discussion" section).

Identification of Genes Whose Expression Levels Are Significantly Changed upon Loss of Nucleostemin

To systematically examine the effect of the loss of nucleostemin on gene expression in ES cells, we performed DNA microarray analysis to screen for genes upregulated or downregulated during reduction of nucleostemin expression. By 96 hours, 509 transcripts were enriched in nucleostemin-deficient cells, while 191 transcripts were downregulated. All differentially expressed genes are classified by functional annotation using Gene Ontology database (supporting information Fig. 3). From the analyses of Gene Ontology terms related to the "Biological Process," we confirmed that genes acting negatively on cell proliferation are enriched in upregulated genes upon loss of nucleostemin. We also found that genes involved in regulation of transforming growth factor beta receptor signaling pathway and cell differentiation are upregulated, while genes involved in defense response to bacterium are downregulated upon loss of nucleostemin. Upregulated genes with known specific "Molecular Function" included the leukotriene B4 receptors. To validate the array data, real-time PCR was performed using Taqman probes with respect to seven different genes whose expression levels appeared to be significantly changed in the DNA microarray analyses. In all cases, we observed a remarkable correlation in gene expression level between real-time PCR and array data (supporting information Table 1).

We also looked for gene expressions of p53-downstream genes from the DNA microarray data. Among the 61 known p53-downstream genes, we found that 43 genes are "Present"

(according to the microarray manufacturer's definition) in nucleostemin null ES cells, while the remaining 18 genes are "Absent". Among these 43 expressed genes, we found that 21 genes including *Gadd45*, *Mdm2*, and *p21* genes are significantly upregulated (more than twofold), whereas none of the genes are downregulated to 50% level upon nucleostemin loss (supporting information Table 2), corroborating our finding shown in Figure 4 that overall activity of p53 is elevated in nucleostemin null ES cells, supporting information Table 3 demonstrated that expression levels of most undifferentiated ES marker genes are not significantly changed upon loss of nucleostemin except for *Sox15*.

Effect of Loss of Nucleostemin on ES Cell-Derived Neural Stem/Progenitor Cells

To assess the function of nucleostemin in neural stem/progenitor cells, *nucleostemin*^{-/-}; *Rosa26-NS* ES cells were differentiated into neuronal lineage cells in the absence of doxycycline [28] and neural stem/progenitor cells were obtained [29]. After several passages under conditions for maintaining neural stem/progenitor state, cells were split into two cell populations and cultured with or without doxycycline. Although a decrease in growth rate due to the presence of doxycycline became evident at day 4 (Fig. 6A), the cells became confluent at day 9 (data not shown). The cells could be expanded for multiple passages in the presence of doxycycline with no further deterioration in proliferation rate or cell viability (data not shown). These results were in marked contrast to those obtained with ES cells, in which loss of nucleostemin is detrimental.

Before determining the levels of cell growth and apoptosis, we examined whether the doxycycline-treated neural stem/progenitor cells maintained stem cell state by immunocytochemical analysis using an anti-nestin antibody. All doxycycline-treated and untreated cells express the neural stem/progenitor cell marker nestin [40] in the cytoplasm (Fig. 6B). We also examined by RT-PCR the expression of other neural stem/progenitor maker genes, including *Musashi1* [41] and

STEM CELLS

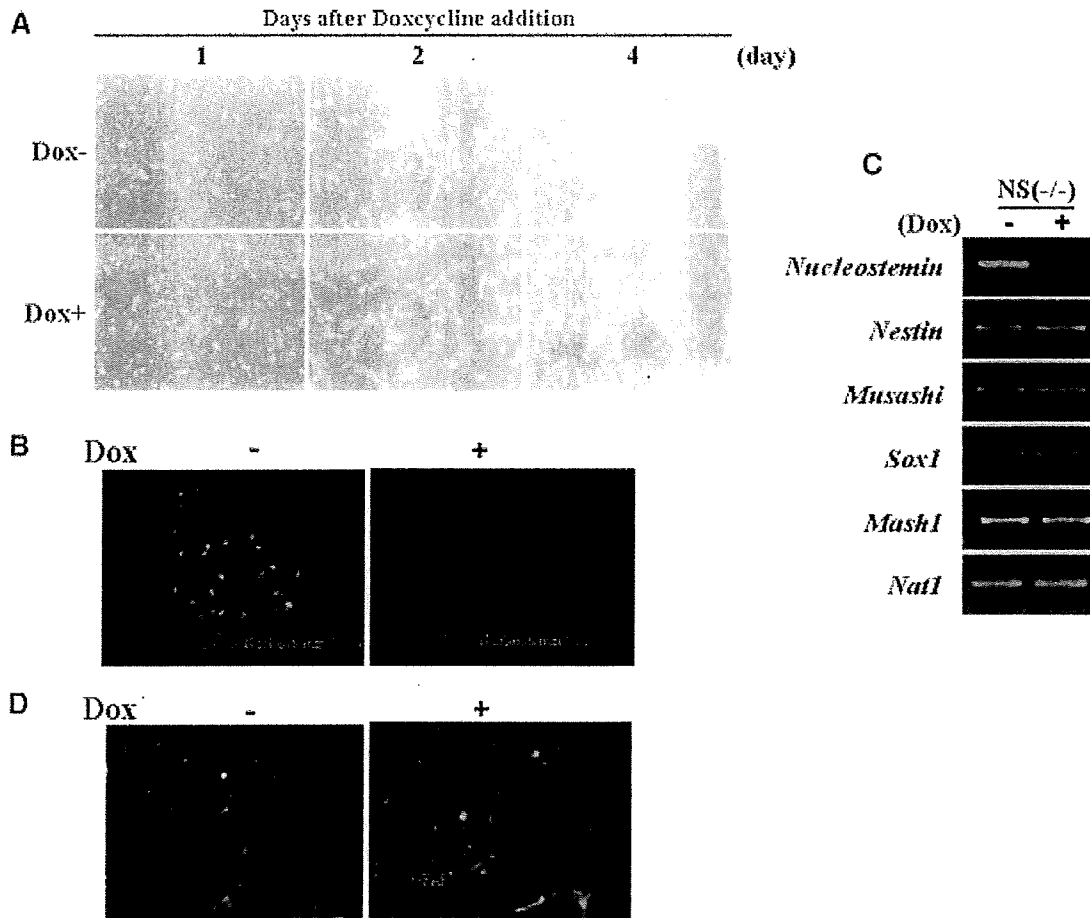


Figure 6. Loss of nucleostemin in embryonic stem (ES) cell-derived neural stem/progenitor cells. (A): Microscopic inspection of *nucleostemin*^{-/-}; *Rosa26-NS* ES cell-derived neural stem/progenitor cells. Neural stem/progenitor cells were obtained using *nucleostemin*^{-/-}; *Rosa26-NS* ES cells as a starting material. After transfer, cells were grown with or without doxycycline and photographs were taken on the indicated days. (B): Preservation of nestin expression in nucleostemin null neural stem/progenitor cells. *Nucleostemin*^{-/-}; *Rosa26-NS* neural stem/progenitor cells were immunostained with anti-nucleostemin and anti-nestin antibodies. Cells were counterstained with DAPI. (C): Maintenance of neural stem/progenitor marker gene expression in the absence of nucleostemin. *Nucleostemin*^{-/-}; *Rosa26-NS* neural stem/progenitor cells were cultured in the presence or absence of doxycycline for 4 days and total RNA was prepared from the cells. Semiquantitative reverse transcription polymerase chain reaction was then performed to examine expression of the indicated genes. (D): Bipotency of nucleostemin null neural stem/progenitor cells. Doxycycline-treated (4 days) and untreated *nucleostemin*^{-/-}; *Rosa26-NS* neural stem/progenitor cells were transferred onto coverslips coated with poly-D-lysine and laminin. After cell attachment, cells were differentiated using 1 μM retinoic acid and 1% fetal bovine serum for 7 days. Doxycycline-treated or untreated conditions were maintained during differentiation. Abbreviations: DAPI, 4',6'-diamidino-2-phenylindole; DOX, doxycycline; GFAP, glial fibrillary acidic protein; MAP2, microtubule-associated protein 2; NS, nucleostemin.

Sox1 [28], and found that they were expressed in both doxycycline-treated and untreated cells, suggesting that as in ES cells, the stem cell state of neural stem cells is not impaired by the loss of nucleostemin. We also confirmed that the ES cell-pluripotent marker *Oct-3/4* was not expressed in these cells (data not shown), although the neural progenitor gene *Mash1* [42] was detected in both cell populations (Fig. 6C).

As the definitive functional attribute of neural stem/progenitor cells is their capacity to generate neurons and glial cells upon differentiation [43, 44], we next examined whether nucleostemin null neural stem cells retain their bipotency. Doxycycline-treated and untreated neural stem/progenitor cells were differentiated with 0.1 μM retinoic acid and 1% fetal bovine serum for 5 days and examined by immunocytochemistry. As shown in Figure 6D, doxycycline-treated and untreated cells converted to neurons and astrocytes at compar-

able efficiencies, further strengthening the idea that as in ES cells, loss of nucleostemin does not lead to the impairment of stem cell state of neural stem cells.

Next, we examined the cell proliferation and apoptosis level in nucleostemin null neural stem cells. The effect of nucleostemin loss on cell proliferation rate is comparable between ES cells and neural stem/progenitor cells, as assayed by BrdU incorporation (compare Figs. 3B, 7A), suggesting that the differential effect of nucleostemin deficiency on ES cells and neural stem cells does not involve a cell proliferation defect, but a cell death defect. At first, we assessed apoptotic cells by annexin V staining and found that no significant difference was evident between doxycycline-treated (9.4%) and doxycycline-untreated cell populations (9.1%). We also quantitated cells of early apoptotic stage (negative for PI) in both cell populations and we found that, again, no

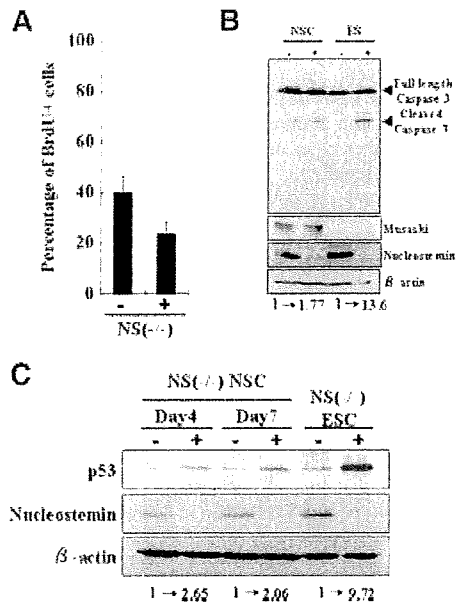


Figure 7. Slight elevation in the levels of activated caspase-3 and p53 in nucleostemin null neural stem/progenitor cells. (A): Cell proliferation defect of nucleostemin null neural stem/progenitor cells. *Nucleostemin*^{-/-}; *Rosa26-NS* neural stem/progenitor cells were cultured in the presence or absence of doxycycline for 4 days, then treated with BrdU for 30 minutes. Incorporation of BrdU was determined by immunocytochemistry and quantified as in Figure 3B. (B): Activation of caspase-3 upon loss of nucleostemin expression is less significant in neural stem/progenitor cells than in ES cells. *Nucleostemin*^{-/-}; *Rosa26-NS* NSC and ES cells were cultured in the presence or absence of doxycycline for 4 days and extracts from these cells were used for western blot analysis with anti-Caspase-3, anti-Musashi, anti-nucleostemin, and anti-β-actin antibodies. (C): *Nucleostemin*^{-/-}; *Rosa26-NS* neural stem/progenitor cells were cultured in the presence or absence of doxycycline for the indicated days, and extracts from these cells were used for western blot analysis using anti-p53, anti-nucleostemin, and anti-β-actin antibodies. Extracts from *nucleostemin*^{-/-}; *ROSA26-NS* ES cells with or without 4 days of doxycycline treatment were used as controls. Abbreviations: BrdU, 5-Bromo-2'-deoxyuridine; ESC, embryonic stem cell; NS, nucleostemin; NSC, neural stem/progenitor cells.

significant change (2.7% vs. 2.4%) was evident (data not shown). In the case of ES cell death, our data indicate that there are caspase-3 dependent and independent pathways accompanied by the loss of nucleostemin. As the molecular basis of caspase-3 independent pathways operating in nucleostemin null ES cells and neural stem/progenitor cells are completely unknown at present, we cannot assess the contribution of those pathways to the cell death of nucleostemin-null neural stem/progenitor cells. Therefore, we examined the level of the activated caspase-3 in neural stem/progenitor cells. As shown in Figure 7B, lanes 1 and 2, although the background level of activated caspase-3 is relatively high in neural stem/progenitor cells, downregulation of nucleostemin results in only a marginal increase in activated caspase-3. This is in marked contrast to results obtained with ES cells, which normally show very low levels of activated caspase-3: upon elimination of nucleostemin expression, activated caspase-3 levels were highly elevated (Fig. 7B, lanes 3 and 4).

As we detected prominent accumulation of the protein in ES cells, we also examined the level of p53 accumulation in

neural stem/progenitor cells. However, unlike ES cells, neural stem/progenitor cells showed only a marginal increase in p53 levels (Fig. 7C). Thus, these results suggest that the milder effect of nucleostemin loss in neural stem/progenitor cells than in ES cells on cell viability is at least in part due to reduced induction of activated caspase-3 and/or p53.

To assess the effect of nucleostemin loss in gene expression in neural stem/progenitor cells, we performed real-time PCR analyses with genes, which are significantly affected by nucleostemin loss in ES cells. From these analyses, we found that, unlike the cases of ES cells, no significant change or only marginal change in gene expression was evident in all cases except for nucleostemin itself (supporting information Table 1). These results indicate that nucleostemin, albeit its expression is comparable between ES cells and neural stem/progenitor cells, affects gene expression network rather specifically in ES cells. Thus, it is possible to assume that the changes in gene expression coupled to nucleostemin loss underlie the observed detrimental cellular phenotype in ES cells.

DISCUSSION

Nucleostemin is expressed in many types of stem cells, including ES cells, neural stem cells, and hematopoietic stem cells [11, 12, 14]. High levels of nucleostemin expression are also detected in several types of cancer cells [16–18]. Although the role of nucleostemin in U2OS human osteosarcoma cells has been assessed extensively by siRNA-mediated knockdown experiments, the physiological function of nucleostemin in stem cells has been little characterized, with the exception of a few studies [15, 45]. Here, we assessed the roles of nucleostemin in ES cells and ES cell-derived neural stem cells. Our data demonstrate that loss of nucleostemin does not affect the expression of pluripotency markers such as Oct-3/4 and UTF1. This result is in accord with the previous observation that strong Oct-3/4 expression is preserved in the inner cell mass of nucleostemin null blastocysts [12]. Furthermore, our data demonstrate that, as in ES cells, the stem cell state of neural stem/progenitor cells is not affected by the loss of nucleostemin. Expression of the neural stem/progenitor cell marker genes Sox1, nestin, and Musashi, and bipotency (generation of both neurons and glial cells upon induction of differentiation) are maintained in the absence of nucleostemin. Our data also demonstrate that, as in cancer cells [16–18] and inner cell mass cells [12, 13], nucleostemin is involved in cell cycle progression and prevention of apoptosis in ES cells and neural stem/progenitor cells.

The most significant finding of this report is the differential requirement for nucleostemin of ES cells and neural stem/progenitor cells for cell viability. Indeed, our data demonstrate that loss of nucleostemin in ES cells results in loss of cell viability over long-term culture, whereas the viability of nucleostemin null neural stem/progenitor cells can be sustained for more than 10 passages without losing neural stem cell marker expression and bipotency. The severe effect of loss of nucleostemin on the viability of ES cells is rather unexpected, because it has been previously demonstrated by immunohistochemical staining with antiactivated caspase-3 antibody that very few, if any, dying cells are detected both in wild-type and nucleostemin null blastocysts [12]. There are two possible explanations that may account for this apparent discrepancy. Our data demonstrate that there are at least two different apoptotic pathways operating in ES cells: one that is dependent on activated caspase-3 and the other independent.

As the previous study examining the inner cell mass of nucleostemin null blastocysts only counted the number of activated caspase-3-positive cells [12], it is possible that a caspase-independent apoptotic pathway is even more prominently activated in nucleostemin null cells. This idea is supported by the fact that the forced expression of Bcl-2 reduced the production of activated caspase-3, but failed to even partially rescue the cell death phenotype in nucleostemin null cells. The second possibility, which is not mutually exclusive to the first possibility, is that a cell viability defect only becomes apparent by rigorous testing, which includes relatively long-term culture *in vitro*, whereas short-term embryogenesis (upto 4.0 d.p.c.) *in utero* is not sufficient to reveal an obvious defect.

The molecular basis of the different phenotypes associated with nucleostemin loss in ES cells and neural stem/progenitor cells is not known at present. Elevated p53 and activated caspase-3 protein levels as a result of nucleostemin loss are more profound in ES cells than in neural stem/progenitor cells, suggesting that these factors are at least partly involved in the ES cell phenotype. Consistent with this idea, we could rescue this detrimental phenotype of nucleostemin null ES with a p53 inhibitor Pifithrin- α , albeit incompletely. Partial, but not complete, rescue with Pifithrin- α implicates that p53-independent pathways, whose molecular bases are currently unknown, may participate in the cell death of nucleostemin null ES cells. Another possibility, which is not mutually exclusive with the above possibility, is that Pifithrin- α exerts a certain side-effect other than inhibiting p53 activity which may affect ES cell viability. Consistent with this notion, we found that treatment with higher concentrations (e.g., 30 μ M) of Pifithrin- α fairly reduced the rescue efficiency (data not shown). Unlike the case of Pifithrin- α treatment, the forced expression of Bcl-2 in nucleostemin null ES cells to inhibit caspase-dependent apoptosis did not lead to even partial recovery of cell viability, implying that caspase-independent pathways also contributed significantly to the death of ES cells. A number of reports have described caspase-independent cell death, including induction by HtrA2/Omi [46] or apoptosis inducing factor [47]. However, it appears that the different types of caspase-independent cell death do not share an underlying cause, except for the fact that the detrimental phenomena cannot be prevented by pharmacological or genetic inactivation of caspases [48, 49]. Therefore, we do not know what cell death pathway operates in nucleostemin null ES cells. As it is also known that inhibition of caspase often leads to a shift from typical apoptosis to nonapoptotic pathways, overexpression of

Bcl-2 in nucleostemin null ES cells may simply cause a switch from one cell death pathway to another.

In any event, our future studies will aim at understanding the molecular basis of the nucleostemin null ES cell phenotype. We will also aim at unraveling the physiological roles of nucleostemin in other types of stem cells, such as hematopoietic stem cells and mesenchymal stem cells, as well as cancer cells and cancer stem cells, by cell type-specific gene disruption.

SUMMARY

In summary, we have generated ES cells in which both alleles of nucleostemin are disrupted, but nucleostemin cDNA is introduced into the *Rosa26* locus together with the Tet off system. Using this ES cell line, we demonstrated that nucleostemin is involved in progression of the cell cycle and prevention of apoptosis both in ES cells and neural stem/progenitor cells. Our data also indicate that loss of nucleostemin results in a much more severe phenotype in ES cells than in neural stem/progenitor cells.

ACKNOWLEDGMENTS

We thank Drs. Hitoshi Niwa and Yutaka Nakachi for providing ERBTcH3 ES cells and helping with functional annotation analyses, respectively, and Daisuke Horiuchi, Mai Kitazato, and Tomoko Okuda for their excellent technical assistance. We are also indebted to Drs. Satoru Miyagi and Takehisa Sakaguchi for helpful discussions. This work was supported in part by the Ministry of Education, Culture, Sports, Science and Technology of Japan. This work was also performed as part of the Core Research for Evolutional Science and Technology (CREST) project supported by the Japan Science and Technology Agency. J.N. is a recipient of fellowship from Nagai Foundation, Tokyo. J.N. is currently affiliated with the Department of Neuroscience, Johns Hopkins University School of Medicine, Baltimore, MD.


DISCLOSURE OF POTENTIAL CONFLICTS OF INTEREST

The authors indicate no potential conflicts of interest.

REFERENCES

- Rossi DJ, Jamieson CH, Weissman IL. Stem cells and the pathways to aging and cancer. *Cell* 2008;132:681–696.
- Ivanova NB, Dimos JT, Schaniel C et al. A stem cell molecular signature. *Science* 2002;298:601–604.
- Ramalho-Santos M, Yoon S, Matsuzaki Y et al. "Stemness": Transcriptional profiling of embryonic and adult stem cells. *Science* 2002;298:597–600.
- Mikkers H, Frisen J. Deconstructing stemness. *EMBO J* 2005;24:2715–2719.
- Eckfeldt CE, Mendenhall EM, Verfaillie CM. The molecular repertoire of the "almighty" stem cells. *Nat Rev Mol Cell Biol* 2005;6:726–737.
- Avillion AA, Nicolis S, Pevny LH et al. Multipotent cell lineages in early mouse development depend on SOX2 function. *Genes Dev* 2003;17:126–140.
- Taranova OV, Magness ST, Fagan BM et al. SOX2 is a dose-dependent regulator of retinal neural progenitor competence. *Genes Dev* 2006;20:1187–1202.
- Cavallaro M, Mariani J, Lancini C et al. Impaired generation of mature neurons by neural stem cells from hypomorphic Sox2 mutants. *Development* 2008;135:541–557.
- Galan-Cardiad JM, Harel S, Arenzana TL et al. Zfx controls the self-renewal of embryonic and hematopoietic stem cells. *Cell* 2007;129:345–357.
- Sakaguchi T, Nishimoto M, Miyagi S et al. Putative "stemness" gene Jam-B is not required for maintenance of stem cell state in embryonic, neural, or hematopoietic stem cells. *Mol Cell Biol* 2006;26:6557–6570.
- Tsai RY, McKay RD. A nucleolar mechanism controlling cell proliferation in stem cells and cancer cells. *Genes Dev* 2002;14:1439–1447.
- Beekman C, Nichane M, Clercq SD et al. Evolutionarily conserved role of nucleostemin: Controlling proliferation of stem/progenitor cells during early vertebrate development. *Mol Cell Biol* 2006;26:9291–9301.
- Zhu Q, Yasumoto H, Tsai RYL. Nucleostemin delays cellular senescence and negatively regulates TRF1 protein stability. *Mol Cell Biol* 2006;26:9279–9290.
- Meng L, Zhu Q, Tsai RYL. Nucleolar trafficking of nucleostemin family proteins: Common versus protein-specific mechanisms. *Mol Cell Biol* 2007;27:8670–8682.

- 15 Kafienah W, Mistry S, Williams C et al. Nucleostemin is a marker of proliferating stromal stem cells in adult human bone marrow. *Stem Cells* 2006;24:1113–1120.
- 16 Liu SJ, Cai ZW, Liu YJ et al. Role of nucleostemin in growth regulation of gastric cancer, liver cancer and other malignancies. *World J Gastroenterol* 2004;10:1246–1249.
- 17 Ma H, Pederson T. Depletion of the nucleolar protein nucleostemin causes G1 cell cycle arrest via the p53 pathway. *Mol Biol Cell* 2007;18:2630–2635.
- 18 Dai MS, Sun XX, Lu H. Aberrant expression of nucleostemin activates p53 and induces cell cycle arrest via inhibition of MDM2. *Mol Cell Biol* 2008;28:4365–4376.
- 19 Mouniford P, Zevnik B, Duwel A et al. Dicistronic targeting constructs: Reporters and modifiers of mammalian gene expression. *Proc Natl Acad Sci USA* 1994;91:4303–4307.
- 20 Masui S, Shimosato D, Toyooka Y et al. An efficient system to establish multiple embryonic stem cell lines carrying an inducible expression unit. *Nucleic Acids Res* 2005;33:e43.
- 21 Araki K, Imaizumi T, Okuyama K et al. Efficiency of recombination by Cre transient expression in embryonic stem cells: Comparison of various promoters. *J Biochem* 1997;122:977–982.
- 22 Alexopoulou AN, Couchman JR, Whiteford JR. CMV early enhancer/chicken beta actin (CAG) promoter can be used to drive transgene expression during the differentiation of murine embryonic stem cells into vascular progenitors. *BMC Cell Biol* 2008;9:2.
- 23 Tomioka M, Nishimoto M, Miyagi S et al. Identification of Sox-2 regulatory region which is under the control of Oct-3/4-Sox-2 complex. *Nucleic Acids Res* 2002;30:3202–3213.
- 24 Thomas KR, Capecchi MR. Site-directed mutagenesis by gene targeting in mouse embryo-derived stem cells. *Cell* 1987;51:503–512.
- 25 Okuda A, Fukushima A, Nishimoto M et al. UTF1, a novel transcriptional coactivator expressed in pluripotent embryonic stem cells and extra-embryonic cells. *EMBO J* 1998;17:2019–2031.
- 26 Miyagi S, Saito T, Mizutani K et al. The Sox-2 regulatory regions display their activities in two distinct types of multipotent stem cells. *Mol Cell Biol* 2004;24:4207–4220.
- 27 Okamoto K, Okazawa H, Okuda A et al. A novel Octamer binding transcription factor is differentially expressed in mouse embryonic cells. *Cell* 1990;60:461–472.
- 28 Ying QL, Stavridis M, Griffiths D et al. Conversion of embryonic stem cells into neuroectodermal precursors in adherent monoculture. *Nat Biotechnol* 2003;21:183–186.
- 29 Conti L, Pollard SM, Gorba T et al. Niche-independent symmetrical self-renewal of a mammalian tissue stem cell. *Plos Biol* 2005;3:e283.
- 30 Yamanaka S, Zhang XY, Maeda M et al. Essential role of NAT1/p97/DAP5 in embryonic differentiation and the retinoic acid pathway. *EMBO J* 2000;19:5533–5541.
- 31 Nishimoto M, Fukushima A, Miyagi S et al. Structural analyses of the UTF1 gene encoding a transcriptional coactivator expressed in pluripotent embryonic stem cells. *Biochem Biophys Res Commun* 2001;285:945–953.
- 32 Niwa H. How is pluripotency determined and maintained? *Development* 2007;134:635–646.
- 33 Mayford M, Bach ME, Huang Y-Y et al. Control of memory formation through regulated expression of a CaMKII transgene. *Science* 1996;274:1678–1683.
- 34 Nishimoto M, Miyagi S, Yamagishi T et al. Oct-3/4 maintains the proliferative embryonic stem cell state via specific binding to a variant Octamer sequence in the regulatory region of the UTF1 locus. *Mol Cell Biol* 2005;25:5084–5094.
- 35 Haupt Y, Maya R, Kazaz A et al. Mdm2 promotes the rapid degradation of p53. *Nature* 1997;387:296–299.
- 36 Kubbutat MH, Jones SN, Vousden KH. Regulation of p53 stability by Mdm2. *Nature* 1997;387:299–303.
- 37 Miyashita T, Reed JC. Tumor suppressor p53 is a direct transcriptional activator of the human bax gene. *Cell* 1995;80:293–299.
- 38 Schmidt T, Komer K, Karsunky H et al. The activity of the murine Bax promoter is regulated by Sp1/3 and E-box binding proteins but not by p53. *Cell Death Differ* 1999;6:873–882.
- 39 Komarov PG, Komarova EA, Kondratov RV et al. A chemical inhibitor of p53 that protects mice from the side effects of cancer therapy. *Science* 1999;285:1733–1737.
- 40 Josephson R, Muller T, Pickel J et al. Pou transcription factors control expression of Cns stem cell-specific gene. *Development* 1998;125:3087–3100.
- 41 Sakakibara S, Nakamura Y, Yoshida T et al. RNA-binding protein Musashi family: Roles for CNS stem cells and a subpopulation of endothelial cells revealed by targeted disruption and antisense ablation. *Proc Natl Acad Sci USA* 2002;99:15194–15199.
- 42 Parras CM, Schuurmans C, Scardigli R et al. Divergent functions of the proneural genes Mash1 and Ngn2 in the specification of neuronal subtype identity. *Genes Dev* 2002;16:324–338.
- 43 Davis AA, Temples S. A self-renewing multipotential stem cell in embryonic rat cerebral cortex. *Nature* 1994;372:263–266.
- 44 Glaser T, Pollard SM, Smith A et al. Tripotent differentiation of adherently expandable neural stem (NS) cells. *Plos One* 2007;3:e298.
- 45 Jafarnejad SM, Mowla SJ, Matin MM. Knocking-down the expression of nucleostemin significantly decreases rate of proliferation of rat bone marrow stromal stem cells in an apparently p53-independent manner. *Cell Prolif* 2008;41:28–35.
- 46 Trencia A, Fiory F, Maitan MA et al. Omi/HtrA2 promotes cell death by binding degrading the antiapoptotic protein ped/pea-15. *J Biol Chem* 2004;279:46566–46572.
- 47 Joza N, Susin SA, Daugas E et al. Essential role of the mitochondrial apoptosis-inducing factor in programmed cell death. *Nature* 2001;410:549–554.
- 48 Abraham MC, Shiham S. Death without caspase, caspase without death. *Trends Cell Biol* 2004;14:184–193.
- 49 Kroemer G, Martin SJ. Caspase-independent cell death. *Nat Med* 2005;11:725–730.

 See www.StemCells.com for supporting information available online.

Significance of Lavage Cytology in Advanced Gastric Cancer Patients

Takeo Fukagawa · Hitoshi Katai · Makoto Saka ·
Shinji Morita · Yuko Sasajima · Hirokazu Taniguchi ·
Takeshi Sano · Mitsuru Sasako

Published online: 7 January 2010
© Société Internationale de Chirurgie 2010

Abstract

Background Lavage cytology positive (Cy1) is well known as a poor prognostic factor in advanced gastric cancer patients. However, the optimal therapeutic strategy for patients with Cy1 has not yet been established. The aim of this study was to evaluate the clinical significance of Cy1 for the purpose of establishing a suitable therapeutic strategy.

Methods The data of 996 consecutive advanced gastric cancer patients who underwent gastrectomy between 1992 and 1998 at the National Cancer Center Hospital were retrospectively studied.

Results The 2- and 5-year survival rates of the patients who underwent gastrectomy without any other noncurative factors besides Cy1 were 25.3 and 7.8%, respectively. When the analysis was limited to type 4 advanced gastric cancer patients, none of the patients with Cy1 survived for more than 40 months.

Conclusions The prognosis of gastric cancer patients with Cy1 is very poor. Some patients show long survival after standard gastrectomy with D2 lymph node dissection;

however, the prognosis of type 4 gastric cancer patients with Cy1 is so poor that multimodality therapy, including perioperative chemotherapy, is essential.

Introduction

Recently, standard therapeutic strategies have been established for gastric cancer patients based on the results of some clinical trials [1–3]. The treatment outcomes of early gastric cancer patients are now favorable [4] due to the remarkable progress in endoscopic treatments [5, 6] and minimally invasive surgery, including function-preserving gastrectomy [7] and laparoscopic gastrectomy [8]. However, many surgeons believe that the treatment outcomes of advanced gastric cancer patients remain poor.

Peritoneal dissemination is one of the most frequent modes of metastasis in advanced gastric cancer. The possibility of cure in patients with this metastasis is considered to be low because no effective curative therapy has been established so far. Even after curative surgery in patients without evidence of peritoneal dissemination at the time of the operation, many patients develop peritoneal recurrence, which is extremely difficult to overcome [9].

The majority of patients showing lavage cytology-positive (Cy1) intraoperatively develop peritoneal recurrence [9]. Cy1 can be interpreted as a state in which free cancer cells are floating in the abdominal cavity, with small peritoneal foci already established in the peritoneum [10]. However, despite Cy1 being recognized as a definite predictive factor for peritoneal recurrence of gastric cancer [11–13], no effective treatment strategies have been established for Cy1 gastric cancer patients. In some cases prolonged survival has been achieved, even in Cy1 patients. When the analysis is limited to patients with type

T. Fukagawa (✉) · H. Katai · M. Saka · S. Morita
Gastric Surgery Division, National Cancer Center Hospital,
5-1-1 Tsukiji, Chuo-ku, Tokyo 104-0045, Japan
e-mail: tfukagaw@ncc.go.jp

Y. Sasajima · H. Taniguchi
Clinical Laboratory Division, National Cancer Center Hospital,
Tokyo, Japan

T. Sano
Digestive Surgery, Cancer Institute Hospital, Tokyo, Japan

M. Sasako
Digestive Surgery, Hyogo Medical College, Nishinomiya,
Hyogo, Japan

4 advanced gastric cancer, however, the prognosis of Cy1 seems to be particularly severe [14].

In this study, the exact relevance of Cy1 and the clinical outcomes of these patients were evaluated based on data from a large-volume center of gastric cancer patients. This is expected to be helpful for developing a suitable new therapeutic strategy for this condition.

Patients and methods

The data of 996 consecutive patients who underwent gastrectomy between 1992 and 1998 for advanced gastric cancer that invaded the gastric wall deeper than the muscularis propria, as assessed by histopathological examination performed after the surgery at the National Cancer Center Hospital, were studied retrospectively. All patients underwent partial or total gastrectomy with lymph node dissection. Basically, patients with peritoneal dissemination underwent simple gastrectomy with minimum dissection; other patients underwent standard dissection. Patients with preoperative, clinically definitive peritoneal dissemination, i.e., ascites, hydronephrosis, and colonic stenosis by barium enema study, were not included in this study. Both the patients with diffuse peritoneal dissemination detected at surgery and those with locally resectable peritoneal dissemination were included in this study.

The former Japanese Classification of Gastric Carcinoma defined peritoneal dissemination as P0, P1, P2, and P3 according to its extent, while the current classification (13th) is P0 and P1: with or without. All patients were classified according to the Japanese Classification of Gastric Carcinoma. Macroscopic features of advanced gastric cancer are classified as type 0: superficial, flat tumors; type 1: polypoid tumors; type 2: ulcerated tumors; type 3: ulcerated tumors without definite limits; type 4: diffusely infiltrating carcinomas; and type 5: nonclassifiable carcinomas. For the purpose of the present analysis, the patients were divided into two groups based on the macroscopic features of type 4 gastric cancer and others.

Cytopathology

Cytological samples were obtained just after laparotomy. Approximately 100 ml of sterile saline was instilled into the pouch of Douglas and then aspirated. The samples were subjected to cytocentrifugation onto slide glasses at 1700 rpm for 60 s at room temperature. The slides were then fixed in 95% ethanol, followed by Papanicolaou and alcian blue stains. Additional slides were stained immunocytochemically for CEA (Mochida, CEA010, Tokyo, Japan), and also for epithelial antigen using the BerEP4 antibody (DAKOPATTS, Glostrup, Denmark). Two to

three cytotechnologists and cytopathologists independently examined all the slides to arrive at a diagnosis by consensus. A patient was considered to have positive peritoneal cytology (Cy1) if adenocarcinoma cells were detected, regardless of the number of cells. In cases where atypical cells were present but could not be definitely identified as cancer cells, the peritoneal cytology was estimated as class 3, or indeterminate. Basically, lavage cytology was carried out intraoperatively for advanced gastric cancer cases. The data of cytology in this article, recorded in our database, is the final result confirmed by immunohistochemistry several days after surgery.

Statistical analysis

Statistical analysis was carried out using SPSS software version 11.5 (SPSS Inc., Chicago, IL). The Kaplan–Meier method was used for constructing the survival curves, and the log-rank test was used for evaluating the statistical significance of differences between the survival curves.

Results

Among the 996 cases included in our study, cytological examination was performed in 779 (Table 1). Cytological examination was positive for cancer cells mainly in advanced gastric cancer patients in whom the tumor had invaded outside the serosal surface (T3) or directly invaded adjacent organs (T4) (Table 1).

As expected, many of the patients with peritoneal dissemination (P1) were cytology-positive (Cy1) but 27 patients with peritoneal dissemination (P1) were cytology-negative (Cy0) (Table 2).

Among the 996 consecutive patients, 217 patients who did not undergo cytological examination and 13 whose cytological examination revealed an indeterminate result were excluded from the analysis; in addition, 65 patients who had distant metastasis to the liver, lung, and supraclavicular lymph nodes were also excluded. The remaining

Table 1 Correlation between cytological examination and the depth of the tumors

	T2 (MP)	T2 (SS)	T3	T4	Total
Cy0	78	156	251	56	541
Cy1	1	5	137	82	225
Indeterminate	0	0	9	4	12
Undone	105	58	44	10	217
	184	219	441	152	996

MP muscularis propria, SS subserosa, Cy0 cytology-negative, Cy1 cytology-positive